♦ Asynchronous Multicarrier Multiple Access: Optimal and Sub-Optimal Detection and Decoding

Andrea M. Tonello

In this paper, we describe multicarrier multiple access architectures that are based on combining filtered multicarrier modulation with multiplexing of sub-carriers across distinct users. These architectures can be deployed for both uplink and downlink wireless communications. We focus on the more critical uplink where multiple users share an asynchronous channel. Signals belonging to distinct users experience time and carrier frequency asynchronism and propagate through independent frequency-selective fading channels. In such a scenario the receiver sees intersymbol interference, intercarrier interference, and multiple access interference components that are a function of the propagation conditions, the design of the sub-channel transmit filters, and the tone allocation strategy. We formulate the optimal multicarrier multiuser detector that yields minimum probability of error. Then, we devise sub-optimal (simplified) detection approaches. These detectors are soft-in soft-out modules that can be concatenated with the channel decoders when the users' information signals are channel encoded. In such a case, practical decoding can be performed by the iterative concatenation of multicarrier detection and decoding (turbo multiuser decoding).

Introduction

Multicarrier modulation has been widely investigated for application to communication systems with high data rate requirements. Chang originally derived the conditions for the transmission of orthogonal band-limited signals [10]. Weinstein and Ebert proposed the practical implementation through the use of the discrete Fourier transform (DFT) [51]. Hirosaki studied the deployment of filtered multicarrier modulation and its efficient implementation via DFT [19]. Cimini investigated the deployment of orthogonal frequency division multiplexing (OFDM) over a wireless channel [13]. In the context of wireline applications, it has been standardized for the high data rate transmission over the copper pair in the advanced digital subscriber line system (ADSL) [2]. In the context of broadcast wireless applications it as been standardized in the digital audio broadcast system (DAB) [1, 24] and in the digital video broadcast (DVB) system [16]. It has also been standardized for application to wireless local area networks (LAN), e.g., IEEE 802.11a [20] and high-performance radio LAN type 2 (HIPERLAN2) [15]. The main advantage of multicarrier modulation is its high spectral

Bell Labs Technical Journal 7(3), 191–217 (2003) © 2003 Lucent Technologies Inc. Published by Wiley Periodicals, Inc. Published online in Wiley InterScience (www.interscience.wiley.com). • DOI: 10.1002/bltj.10027

efficiency and its proven robustness to frequency-selective channels, i.e., highly time dispersive, where the equalization task is greatly simplified. However, the above proposals are limited to consider respectively the single-user link, the broadcast link, and the multiple access link where the common media is accessed with a time division protocol. More recently, several proposals have considered the combination of multicarrier modulation with code division multiple access (CDMA) for application to cellular mobile communications [23, 47].

In this paper, we investigate the impact of deploying multicarrier modulation in an asynchronous multiple access channel that is shared in a frequency division mode [35]. Distinct users send their information signal to a central receiver and are multiplexed in frequency by assigning them subsets of the available carriers. The multiplexing scheme is referred to as multicarrier multiple access (MC-MA). Further, users are asynchronous, meaning that they have a certain amount of temporal and carrier frequency misalignment with respect to a reference point at the receiver. The time misalignments are due to different propagation delays of users at different distance from the receiver. The carrier frequency offsets are due to misadjusted oscillators and Doppler from users' movement. This model is appropriate to describe the uplink of a mobile wireless communication system such as the uplink of a satellite system, of a wireless LAN (WLAN), or of a mobile cellular system. We assume, in general, propagation through frequency-selective time-variant fading channels. With the appropriate variations, the model can be used also to describe a wireline system where a set of terminals communicates with a central receiver.

In our system implementation, we consider temporal and frequency shaping of the sub-channels by deploying sub-channel transmit filtering. Under certain conditions efficient digital implementation of the transmitters is possible. It is based on fast Fourier transform (FFT) and digital polyphase filtering. In such a case the system is a multiuser extension of filtered multitone modulation (FMT) [12], and we refer to it as filtered multitone multiple access (FMT-MA) [35, 42, 43]. When the sub-channel transmit filters have a rectangular impulse response, the system is referred to as discrete multitone multiple access (DMT-MA) [39–41]. In literature, DMT-MA is also referred to as multiuser orthogonal frequency division multiplexing (OFDM).

In an asynchronous MC-MA wireless system, the receiver sees a multitude of signals that, in general,

Panel 1. Abbreviations, Acronyms, and Terms

1-D—one dimensional
2-D—two dimensional
3-D—three dimensional
ADSL—advanced digital subscriber line
AWGN—additive white Gaussian noise
BCJR—Bahl, Cocke, Jelinek, and Raviv decoding algorithm
BER—bit error rate
CDMA—code division multiple access
DAB—digital audio broadcast
DAC—digital to analog converter
DFT—discrete Fourier transform
DMT-MA—discrete multitone multiple access
FFT—fast Fourier transform
FMT—filtered multitone modulation
HIPERLAN2—high-performance radio LAN type 2
ICI—intercarrier interference
IFFT—inverse FFT
ISI—intersymbol interference
LAN—local area network
MAI—multiple access interference
MAP—maximum a posteriori detection/decoding algorithm
MC-MA—multicarrier multiple access
MIMO—multiple input, multiple output
M-PSK—M-ary phase shift keying modulation
MT-MA—multitone multiple access
OFDM—orthogonal frequency division multiplexing
PSD—iterative per-symbol detection/decoding algorithm
M-QAM—M-ary quadrature amplitude modulation
RAKE receiver—an optimum receiver structure that collects the signal energy from all received signal paths that fall within the span of a given delay line and carry the same information, similar to the action of a garden rake
SNR—signal-to-noise ratio
WLAN—wireless LAN

have propagated through independent frequency-selective fading channels and have relative time offsets and carrier frequency offsets that differ from zero. As a result, intersymbol interference (ISI), intercarrier interference (ICI), and multiple access interference (MAI) components arise. In broadband applications with high coverage and mobility requirements, the users' asynchronism cannot be neglected. Conventional receivers based on single-user detection are unable to provide acceptable performance. Thus, we focus on the problem of deriving the optimal detection algorithm. We pursue the concept of joint detection of signals transmitted over multiple-input multiple-output (MIMO) channels [46]. This approach has found application also in the context of optimal detection of asynchronous CDMA signals [49]. The resulting receiver structure comprises a front-end structure followed by a maximum a posteriori processor that runs the BCJR algorithm [5] with an appropriate metric. Sub-optimal detection based on reduced state methods is also investigated in order to reduce the complexity of the optimal algorithm. The multicarrier-user detectors that we describe are soft-input soft-output modules that can be concatenated in an iterative fashion with the channels decoders when channel coding is deployed. The resulting receiver structure implements a form of turbo multiuser detection and decoding [25].

Little work can be found in literature about this scenario. Some investigation on the timing and carrier frequency synchronization requirements in multiuser pulse-shaped OFDM is presented in [50]. The effect of the time offsets in a DMT-MA system with sub-optimal single-user detection can be found in [21]. A technique for compensating time and frequency misalignments based on feedback control in a DMT-MA system is presented in [45]. On the other hand, a rich body of literature can be found on the study of receivers for DMT modulation in single-user applications in the presence of timing errors, frequency offsets, and multipath fading, e.g., [30, 31] and associated references. An overview of equalization methods for DMT transceivers is presented in [28]. An overview of FMT architectures for broadband digital subscriber lines is given in [12].

Multicarrier Multiple Access Transmission Model

In this section we describe the scheme used to multiplex the users, the transmitter architecture, and the propagation media model.

User Multiplexing

N_U users are multiplexed by allocating M subcarriers (tones) in the available spectrum of width $W = 1/T$. Each user is assigned a subset of such tones according to a given tone allocation strategy. If the subcarriers f_k are uniformly spaced, then we can write (at baseband) $f_k = k/T_1$ with $T_1 = MT$, $k = 0, \ldots, M-1$. Several carrier allocation methods are possible. They play an important role for the optimization of the spectral efficiency, the exploitation of the frequency diversity, and the complexity of the detection algorithm. They can be static or dynamic, orthogonal (i.e., with no sub-carrier collisions) or non-orthogonal. To maximize the spectral efficiency, we could allow for a non-orthogonal scheme where distinct users share some of the sub-carriers. To best exploit the channel frequency diversity, the tones should be distributed across the overall spectrum or be dynamically allocated in accordance to the channel dynamic conditions [11]. The users' asynchronism and the channel frequency selectivity generate multiple access interference at the receiver side. In order to minimize the multiple access interference power levels and simplify the receiver complexity, it is better to allocate trunks of tones that are as far as possible across users.

Some tone allocation strategies (**Figure 1**) are outlined in what follows. With a *block allocation*, each user is assigned a block of K_u contiguous tones; distinct users use distinct blocks. We can insert some guard tones (virtual carriers) between adjacent blocks, thus obtaining a *block allocation with frequency guards*. With an *interleaved allocation*, the tones of the users are regularly interleaved across the overall spectrum. With a *random allocation*, the tones are randomly allocated; the constraint of avoiding the carrier hits can be imposed. With a *dynamic allocation*, the tones are dynamically allocated according to a given pattern; multiplexing of users becomes a sort of multitone frequency hopping [26]. Finally, with an *adaptive allocation*, the tones are assigned according to the channel conditions and interference levels; it requires a

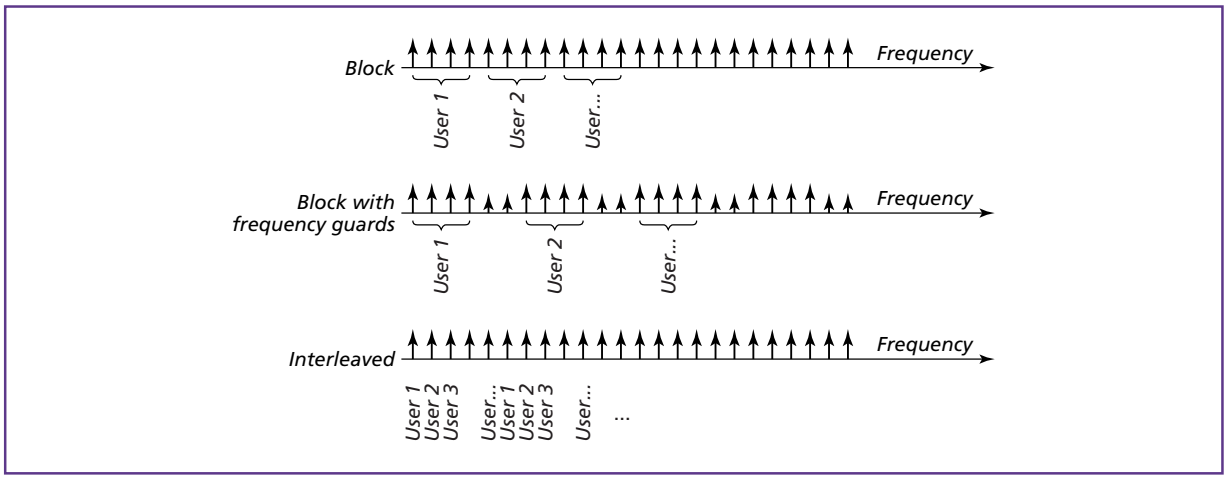

Figure 1.
Tone multiplexing across users.

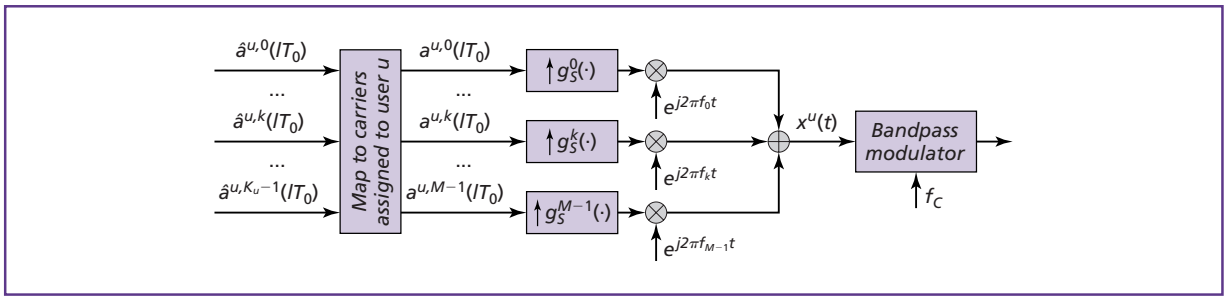

Figure 2.
Analog implementation of the MC-MA transmitter of user u.

feedback control loop from the receiver that monitors the received powers of all users [11].

We note that the multicarrier multiple access scheme that we have described can be applied to both the uplink (terminals-to-base link) and the downlink (base-to-terminals link). However, we focus on the uplink since the asynchronism across users translates into a more critical scenario.

Transmitter

We consider a filter bank implementation of each transmitter (**Figure 2**). The sequence of information bits belonging to user u is mapped into a sequence of complex M-PSK or M-QAM data symbols. Then, it is S/P converted and formatted into M sub-sequences $\{a^{u,k}(lT_0)\}$, $k = 0, \ldots, M-1$, $T_0 = NT$. If K_u is the number of tones assigned to user u, then only K_u out of M sub-sequences differ from zero. Each data sequence is filtered with an interpolation sub-channel filter $g_S^k(t)$ and sub-carrier modulated. The sub-carrier modulator outputs are summed together to obtain the multicarrier lowpass signal of user u. Finally, the lowpass signal is bandpass modulated at RF frequency f_C and transmitted over the air. Note that in general $T_0 \geq T_1$, such that the sub-carriers are non-minimally spaced, which translates into sub-channels with smaller frequency overlapping. If we include the sub-carrier modulator in the transmit filter impulse response, $g_T^k(t) = g_S^k(t)e^{j2\pi f_k t}$, and we define $\tilde{a}^{u,k}(lT_0) = a^{u,k}(lT_0)e^{j2\pi f_k lT_0}$, the lowpass multicarrier signal of user u reads

$$x^u(t) = \sum_{k\in\Gamma_u} \sum_{l=-\infty}^{\infty} \tilde{a}^{u,k}(lT_0) g_T^k(t - lT_0), \qquad (1)$$

where Γ_u is the set of tones indices assigned to user u. In what follows, we assume $g_S^k(t)$ to be identical for

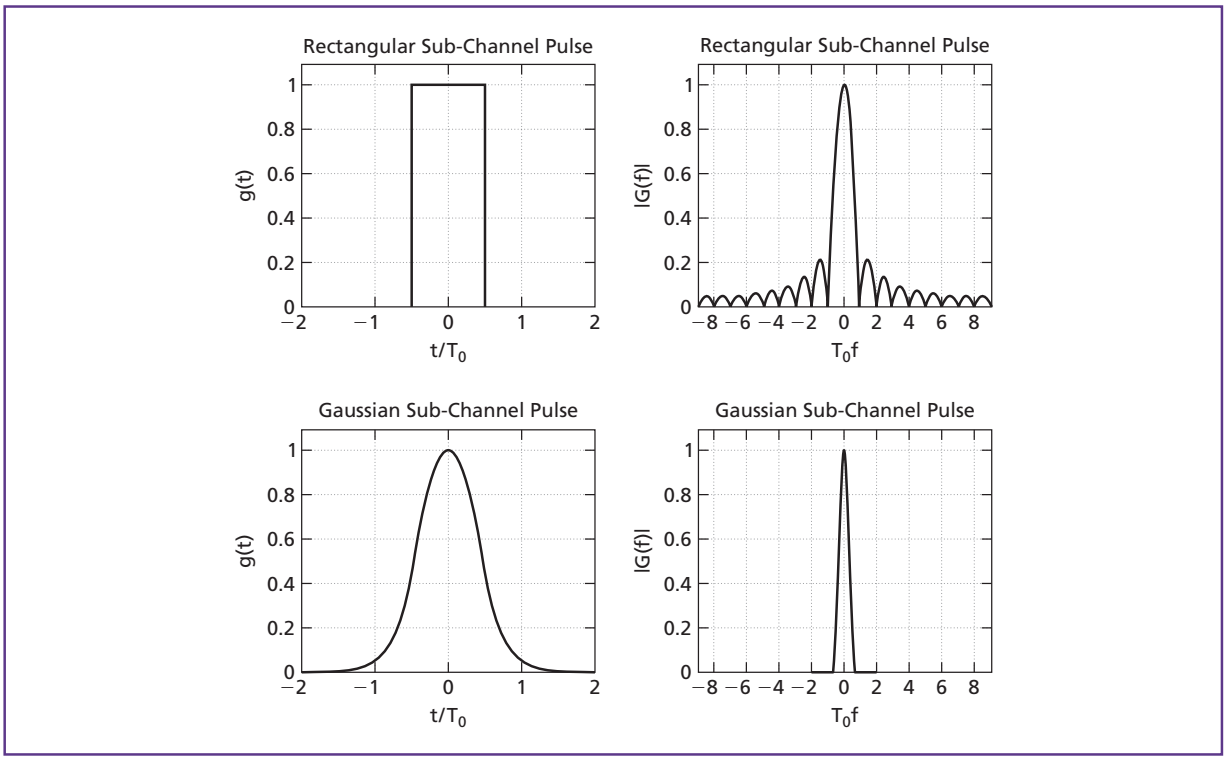

Figure 3.
Impulse and frequency response of rectangular and Gaussian sub-channel pulse.

all sub-channels, i.e., $g_S^k(t) = g_S(t)$, and refer to it as prototype filter.

Prototype Filter

The prototype filter is designed with the goal of minimizing the ICI, ISI, and MAI. In ideal channel conditions, the interference components are nulled if the system is designed in accordance to a generalized Nyquist criterion. Possible choices are to deploy time limited filters, e.g., rectangular filters, $g_S(t) = \mathrm{rect}(t/T_0)$ (**Figure 3**), or band limited filters with ideal rectangular frequency response. Both choices introduce no ISI and no ICI even with minimal sub-carrier spacing that is equal to $1/T_0$. Nyquist filters, e.g., root-raised-cosine sub-channel pulses at both the transmitter and the receiver, do not introduce any ISI in ideal channel conditions; however, the condition of zero ICI is fulfilled when the sub-carrier spacing is larger than $1/T_0$, such that the spectra of adjacent sub-channels do not overlap. In [19] it is shown that the combination of Nyquist filters with an offset-QAM modulation technique can grant zero ISI and ICI with minimal sub-carrier spacing. Another choice that we consider in this paper is to deploy Gaussian-shaped filters, $g_S(t) = \exp(-(\alpha t/T_0)^2)$, with $\alpha = f_{3dB}T_0\pi\sqrt{2/\ln 2}$ (Figure 3). Although they are not Nyquist filters, they have the interesting property of being practically limited in time and in frequency. Real asynchronous channels introduce a certain amount of time dispersion, of time misalignment, and of frequency misalignment, which translates into a loss of system orthogonality. That is, some degree of ISI and ICI is always present. In this respect, the Gaussian filters turn out to be an interesting choice that allows controlling the interference components [22, 35, 42].

Efficient Digital Implementation

Special forms of multicarrier multiple access are obtained when the M parallel information streams

(with data rate $1/T_0$ each) are transmitted over sub-carriers uniformly spaced by $1/T_1$, with $T_1/T_0 = M/N \leq 1$. If we further assume the sub-channel transmit filters to be identical, an efficient implementation of the transmitter comprises a carrier mapping device, an M-point inverse fast Fourier transform (IFFT), followed by a bank of low rate filters that are obtained by the polyphase decomposition of the prototype filter $g_s(nT)$, and a serial to parallel conversion. When the transmit filters are rectangular windows, strictly time limited, the discrete-time system implementation is referred to as discrete multitone multiple access (DMT-MA). When the users transmit their information through filtered/shaped sub-channels that have a limited degree of time and frequency overlapping, the discrete-time implementation is referred to as FMT-MA. It can be viewed as an extension of the FMT modulation concept [6, 12]. Further, the system is referred to as critically and non-critically sampled when the sub-carrier spacing is minimal or non-minimal, respectively. In **Figure 4**, we depict a block diagram of a critically sampled FMT-MA base-band modulator with $N = M$, $T_0 = T_1$, and $g^k(mT_0) = g_S(kT + mT_0)$, $k = 0, \ldots, M-1$.

Asynchronous Multiple Access Channel

In an asynchronous multiple access channel, the signals of distinct users suffer distinct time misalignments and carrier frequency offsets relative to a reference at the receiver. The time offsets are due to the propagation delays of transmitters at different distances from the receiver. The frequency offsets are due to misadjusted oscillators and Doppler from movement. Further, in a wireless uplink scenario, the signals of distinct users propagate through distinct frequency-selective fading channels.

At the receiver side, we first run RF down conversion and lowpass filtering with a broadband filter with nominal bandwidth W. Let $g_E^u(\tau; t)$ be the equivalent lowpass impulse response of user u, at time t, that includes the time-variant channel and the broadband filters in the RF modulator/demodulator. Then, at the receiver side the composite lowpass signal can be written as

$$y(t) = \sum_{u=1}^{N_U} \sum_{k \in \Gamma_u} e^{j(2\pi \Delta f_{u,k} t + \Delta\phi_{u,k})} \sum_{l=-\infty}^{\infty} (\tilde{a}^{u,k}(lT_0) \times g_R^{u,k}(t - lT_0 - \Delta t_{u,k}; t)) + n(t) \quad (2)$$

$$g_R^{u,k}(\tau; t) = \int_R g_T^k(\tau_1) g_E^u(\tau - \tau_1; t) d\tau_1. \quad (3)$$

In (3), $g_R^{u,k}(\tau; t)$ represents the overall time-variant impulse response of the k-th sub-channel of user u that includes the sub-channel transmit filter. In (2), $n(t)$ is the thermal noise contribution that is assumed to be a zero-mean stationary white Gaussian process. The carrier frequency offset of the sub-channel k of user u with respect to the sub-channel carrier frequency of the central receiver is denoted with $\Delta k_{u,k} = f_{C,u} + f_{k,u} - f_C - f_k$ and is assumed smaller than the transmission bandwidth $1/T$. The time offset of the sub-channel k of user u is denoted with $\Delta t_{u,k}$. Finally, $\Delta\phi_{u,k}$ is a phase offset. It should be noted that, although we have assumed distinct time, frequency, and phase offsets for all sub-channels and users, in practical

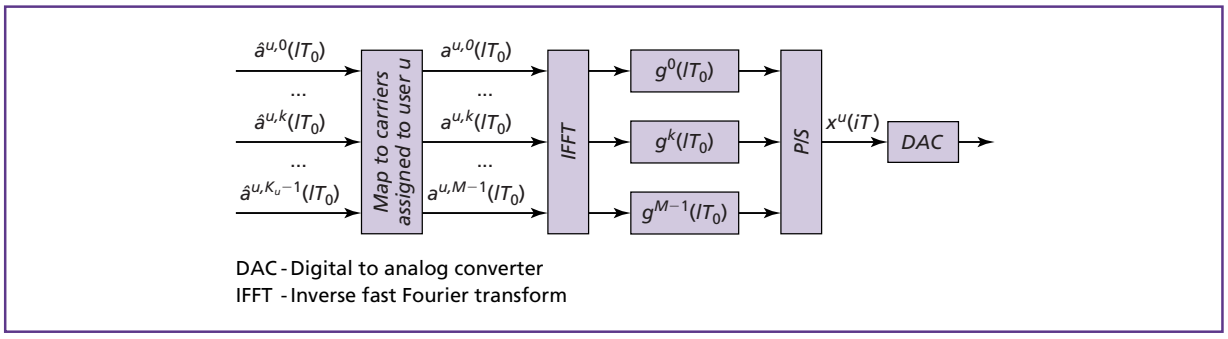

Figure 4.
Discrete time implementation of the critically sampled FMT-MA base-band transmitter of user u.

scenarios they may differ only across distinct users, i.e., $\Delta t_{u,k} = \Delta t_u$, $\Delta f_{u,k} = \Delta f_u$, $\Delta \phi_{u,k} = \Delta \phi_u$ for all indices k. Further, for practical purposes, the frequency-selective fading channel can be modeled with a tapped delay line with a finite number of taps. The tap gains are independent Gaussian distributed with zero mean under the Rayleigh fading assumption.

Multiuser OFDM and Conventional Demodulation

In the MT-MA system architecture that we have described, the sub-channels are in general shaped with a prototype filter. If we deploy rectangular pulses the system is referred to as DMT-MA and often in literature as multiuser OFDM. With reference to the digital implementation, it is well known that in a single-user DMT system (OFDM) simplified detection is implemented by inserting a guard time (cyclic prefix) at the transmitter. Then, the detector simply consists of a stage that disregards the guard time, followed by an FFT module and a one-tap equalizer per-sub-channel. The same detector can be applied in a DMT-MA system. That is, we can acquire carrier and time synchronization with a given user and then run conventional detection. If the guard time is sufficiently long, the ISI channel and the time offsets across users do not generate any interference components although the carrier frequency offsets still cause interference. Clearly, long guard times imply diminished transmission rates. The interested reader is referred to [39–41] where the performance of conventional single-user detection is investigated. This detection approach is quite simple; however, it is sub-optimal and grants acceptable performance only in the presence of small users' asynchronism. Therefore, some form of multiuser detection has to be deployed.

Optimal Demodulation of Multicarrier Multiuser Signals

In this section we devise the optimal demodulation scheme in an asynchronous multicarrier-multiuser system. The goal of the optimal baseband demodulator (detector) is to reconstruct the sequence of transmitted bits/symbols of all users from the observation of the complex lowpass signal $y(t)$ at the output of the receiver front end. This is a problem of jointly detecting multiple received signals. Assuming to observe the received signal over a finite time window $t \in I$, with I sufficiently long such that border effects can be ignored, the optimal detector decides in favor of a transmitted data sequence $\underline{\hat{a}} = \{\hat{a}^{u,k}(lT_0)\}$, $lT_0 \in I$, $u = 1, \ldots, N_U$, $k = 0, \ldots, M-1$, that maximizes, over the set of all possible data sequences, the a posteriori probability

$$P(\underline{a} \,|\, y(t)) = \frac{p(y(t) \,|\, \underline{a})}{p(y(t))} P(\underline{a}). \tag{4}$$

In what follows, we assume the transmitted data symbols to be independent. If coding is applied, this is a reasonable assumption when the coded bits or symbols are interleaved. If no side information is available, the symbols can be considered equally likely, and the decision rule collapses to the maximum likelihood one.

Under the assumption that the additive thermal noise in the transmission medium is a stationary white Gaussian process with double-sided spectral density $2N_0$, the channel probability density function (pdf) conditioned on a given data sequence $\underline{\hat{a}}$, the channel, the frequency offset, and the time offset of all users, is (apart from a constant factor)

$$p(y(t) \,|\, \underline{\hat{a}}) \sim e^{-(1/4N_0)\Omega(\underline{\hat{a}})} \tag{5}$$

$$\Omega(\underline{\hat{a}}) = \int_{t \in I} \left| y(t) - \sum_{u=1}^{N_U} \sum_{lT_0 \in I} \sum_{k=0}^{M-1} \hat{a}^{u,k}(lT_0) e^{j2\pi f_k lT_0} \times e^{j(2\pi \Delta f_{u,k} t + \Delta \phi_{u,k})} g_R^{ik}(t - \Delta t_{u,k} - lT_0; t) \right|^2 dt. \tag{6}$$

We assume, in general, that all M sub-channels can be assigned to each user. The channel pdf (5) is obtained from a generalization of the one reported in [44] for single link (user) transmission and in [46] for multiple channel transmission systems. A generalization of the channel pdf was also used in [49] for the derivation of the MLSE receiver for asynchronous CDMA channels, and more recently in [36] for the derivation of the MAP equalizer in space–time coded systems. The case of correlated noise can also be included as shown in [44].

In the Appendix we show that the *channel log-likelihood function* can be decomposed as follows:

$$\Omega(\underline{\hat{a}}) \sim -\sum_{lT_0 \in I} \sum_{u=1}^{N_U} \sum_{k=0}^{M-1} \Omega^{u,k,l}(\underline{\hat{a}}) \tag{7}$$

$$\begin{aligned}\Omega^{u,k,l}(\underline{\hat{a}}) = \mathrm{Re}\Bigg\{ \hat{a}^{u,k}(lT_0)^* \Bigg(& 2z^{u,k}(lT_0) \\ & - \sum_{u'=1}^{N_U} \sum_{k'=0}^{M-1} \hat{a}^{u',k'}(lT_0) s^{u,u',k,k'}(lT_0, lT_0) \\ & - 2 \sum_{u'=1}^{N_U} \sum_{k'=0}^{M-1} \sum_{l'<I} \hat{a}^{u',k'}(l'T_0) s^{u,u',k,k'}(lT_0, l'T_0) \Bigg) \Bigg\}, \end{aligned} \tag{8}$$

where the *z-parameters* and *s-parameters* (we borrow the terminology z-parameters and s-parameters from [8]) are defined respectively as

$$\begin{aligned} z^{u,k}(lT_0) = & \, e^{-j(2\pi f_k lT_0 + \Delta\phi_{u,k})} \int_I y(t) e^{-j2\pi \Delta f_{u,k} t} \\ & \times g_R^{u,k}(t - \Delta t_{u,k} - lT_0; t)^* dt \end{aligned} \tag{9}$$

$$\begin{aligned} s^{u,u',k,k'}(lT_0, l'T_0) = & \, e^{-j(2\pi(f_k lT_0 - f_{k'} l'T_0) + \Delta\phi_{u,k} - \Delta\phi_{u',k'})} \\ & \times \int_I e^{-j2\pi(\Delta f_{u,k} - \Delta f_{u',k'})t} g_R^{u,k}(t - lT_0 - \Delta t_{u,k}; t)^* \\ & \times g_R^{u',k'}(t - l'T_0 - \Delta t_{u',k'}; t) dt. \end{aligned} \tag{10}$$

If we substitute (5) in (4), under the assumption of the data symbols to be independent with a priori probability $P(\hat{a}^{u,k}(lT_0))$, the a posteriori probability can be factored as follows:

$$P(\underline{\hat{a}} \,|\, y(t)) \sim \prod_{lT_0 \in I} \prod_{u=1}^{N_U} \prod_{k=0}^{M-1} \Bigg(\underbrace{e^{-(1/4N_0)\Omega^{u,k,l}(\underline{\hat{a}})} P(\hat{a}^{u,k}(lT_0))}_{\gamma_l^{u,k}} \Bigg). \tag{11}$$

Therefore, the search of the MAP-transmitted data sequence can be implemented with the BCJR algorithm [5] that uses the transition probabilities $\gamma_l^{u,k}$ defined in (11). From (9), $z^{u,k}(lT_0)$ corresponds to the matched filter output sample of the frequency de-rotated and phase/time-compensated received signal. The filter is matched to the equivalent k-th sub-channel impulse response of user u, and samples are taken at rate $1/T_0$. From (10), $s^{u,u',k,k'}(lT_0, l'T_0)$ is obtained by cross-correlating, with appropriate time offset, frequency offset, and phase offset compensation, the equivalent k-th sub-channel impulse response of user u, with the equivalent k'-th sub-channel impulse response of user u'.

According to (8), cross-terms may be present. They are a function of two symbols transmitted on two given carriers during two signaling periods. These cross-terms are interference components that may be helpful, from a conceptual standpoint, to distinguish as follows:

1. *Intersymbol interference* on sub-carrier k assigned to user u. This is zero if $s^{u,u,k,k}(lT_0, l'T_0) = 0$, for all $l \neq l'$.
2. *Intercarrier interference* between sub-carriers k and k' assigned to user u. This is zero if $s^{u,u,k,k'}(lT_0, l'T_0) = 0$, for all $k \neq k'$ and any pair l, l'.
3. *Multiple-access interference* between sub-carriers k and k', assigned respectively to user u and u', over symbols transmitted at signaling periods lT_0 and $l'T_0$. This is zero if $s^{u,u',k,k'}(lT_0, l'T_0) = 0$ for any pair of distinct users.

These interference components are a function of the prototype filter shape, the sub-carrier spacing and allocation, the channel, and the time/frequency offsets. In order to simplify the multicarrier-user detector, it is desirable that the s-parameters have a duration that is limited in time, i.e., as a function of index l', and in frequency, i.e., as a function of index k'. Clearly, this depends upon the system design and channel characteristics. For instance, if the prototype filters are practically limited in time and frequency, e.g., with Gaussian pulses, and the sub-carriers are appropriately allocated to the users, then the condition of limited cross-correlations can be fulfilled.

It is possible to elaborate further the decomposition (7)–(8) (see the Appendix) if we define the index relations (we denote with a div b and a mod b, respectively, the integer division and the remainder of the integer division)

$$M_1 = MN_U \tag{12}$$

$$\begin{aligned} & m = u + kN_U + lM_1 - 1 \quad u = 1, \ldots, N_U \\ & k = 0, \ldots, M-1 \quad l = -\infty, \ldots, \infty \end{aligned} \tag{13}$$

$$l(m) = m \text{ div } M_1 \tag{14}$$

$$k(m) = (m \bmod M_1) \text{ div } N_U \tag{15}$$

$$u(m) = ((m \bmod M_1) \bmod N_U) + 1. \tag{16}$$

Then, the sequence of data symbols and matched filter outputs can be ordered as follows:

$$\hat{a}_m = \hat{a}^{u(m),k(m)}(l(m)T_0) \quad m = -\infty, \ldots, \infty \tag{17}$$

$$z_m = z^{u(m),k(m)}(l(m)T_0) \quad m = -\infty, \ldots, \infty, \tag{18}$$

and we obtain

$$\Omega(\underline{\hat{a}}) = \sum_m \Omega_m(\underline{\hat{a}}) \tag{19}$$

$$\begin{aligned}\Omega_m(\underline{\hat{a}}) &= \Omega^{u(m),k(m),l(m)}(\underline{\hat{a}}) \\ &= \mathrm{Re}\left\{\hat{a}_m^*\left(2z_m\right.\right. \\ &\quad - \hat{a}_m s^{u(m),u(m),k(m),k(m)}(l(m)T_0, l(m)T_0) \\ &\quad - 2\sum_{n>0}\left(\hat{a}_{m-n}\right. \\ &\quad \left.\left.\left.\times\, s^{u(m),u(m-n),k(m),k(m-n)}(l(m)T_0, l(m-n)T_0)\right)\right)\right\}.\end{aligned} \tag{20}$$

In other words, the log-likelihood function is obtained as the sum of the *transition metrics* (20). Therefore, if we define the *state* as

$$S_{m-1} = \{\hat{a}_{m-1}, \ldots, \hat{a}_{m-L_S}\}, \tag{21}$$

for a finite L_S such that $s^{u(m),u(m-n),k(m),k(m-n)}(l(m)T_0, l(m-n)T_0) = 0$, for $|n| > L_s$, and the *state transition probability* as

$$\gamma_m(S_m, z_m \mid S_{m-1}) \sim \underbrace{e^{-(1/4N_0)\Omega_m(\underline{\hat{a}})}}_{p(z_m \mid S_m, S_{m-1})} \underbrace{P(\hat{a}_m)}_{P(S_m \mid S_{m-1})}, \tag{22}$$

the factorization of the a posteriori probability in (11) becomes

$$P(\underline{\hat{a}} \mid y(t)) \sim \prod_m \gamma_m(S_m, z_m \mid S_{m-1}). \tag{23}$$

That is, the a posteriori probability is factored into the product of the state transition probabilities. In turn, the state transition probability is obtained as the product of the *conditional channel pdf* $p(z_m \mid S_m, S_{m-1})$, with the *a priori transition probability* $P(S_m \mid S_{m-1}) = P(\hat{a}_m)$ between state S_{m-1} and S_m. In general, the transition metric (22) can be used in the BCJR algorithm [5, 18] to calculate the a posteriori probability of the data symbols, the a posteriori probability of the data bits, and the a posteriori probability of a data/bit sequence (see following sections). A block diagram of the baseband processing is depicted in **Figure 5**.

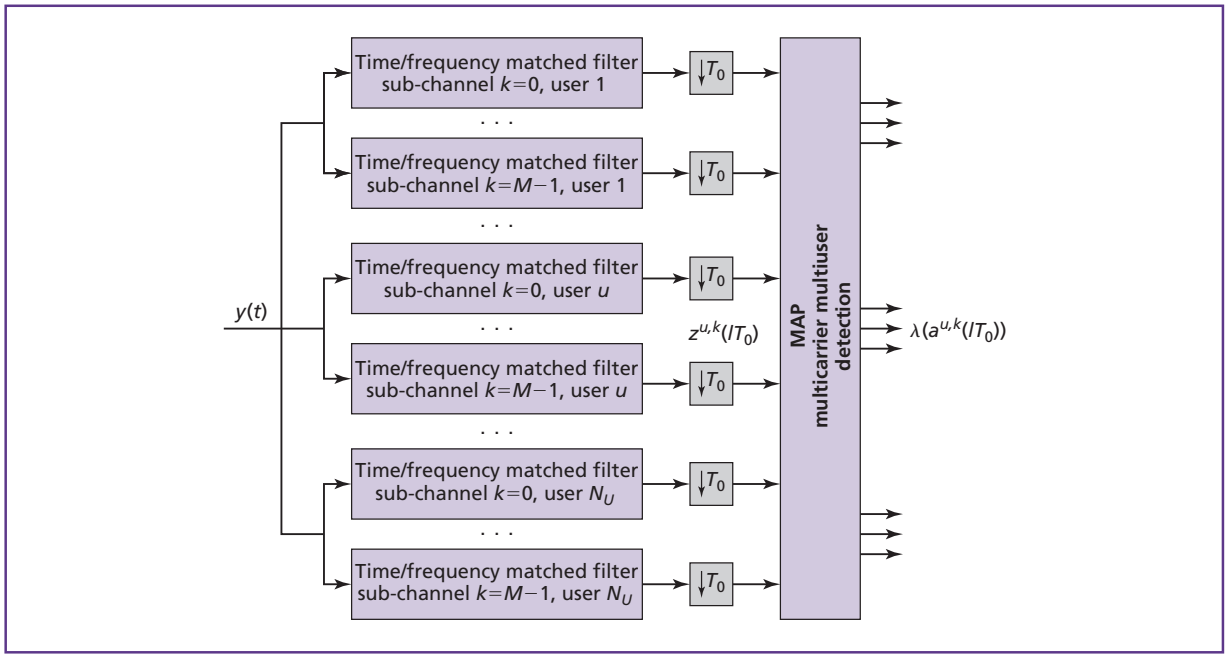

Figure 5.
Optimal multicarrier-multiuser baseband detector.

3-D Markov Chain Representation and Maximum a Posteriori Multicarrier Detection

The factorization in (23) implies that the evolution of the state defined in (21) observed at the sub-channel matched filter outputs can be represented with a Markov chain with transition probabilities defined in (22). It is interesting to note that, when we move on the underlying trellis structure by one step, we increase either the user index, or the sub-carrier index, or the time index. Therefore, the trellis can be imagined as a hyper trellis with a 3-D structure. The trellis has a number of states that is equal to $|\Sigma| = 2^{N_{bps}L_S}$ and a number of transitions to/from each state that is equal to $|\mathrm{T}| = 2^{N_{bps}}$ where N_{bps} is the number of bits per constellation symbol. Note that L_S satisfies the relation $1 \leq L_S \leq MN_U(L_{ch} + 1) - 1$ where L_{ch} is the temporal memory of the sub-channels cross-correlation. The trellis structure essentially determines the complexity of the detection algorithm. Therefore, in general, the complexity grows exponentially with the number bits per constellation symbol, the number of users, the number of sub-carriers, and the channel memory. The actual complexity depends upon the amount of temporal and frequency superposition across the sub-channels. It can be controlled with the appropriate choice of a time-frequency concentrated pulse, and the tone allocation.

The maximum a posteriori algorithm [5, 18] can be used to compute

1. The a posteriori probability of the data symbols (we denote with $\underline{z}$ the sequence of matched filter outputs z_m), i.e.,

$$\begin{aligned}\lambda(a_m = a) &= P(a_m = a \,|\, \underline{z}) \\ &= P(a^{u(m),k(m)}(l(m)\,T_0) = a \,|\, \underline{z}) \end{aligned} \tag{24}$$

   with $a \in A$, and A being the set of all possible data symbols (constellation alphabet).
2. The *a posteriori probability of the data bits*, i.e.,

$$\lambda(d_i = d) = P(d_i = d \,|\, \underline{z}) \tag{25}$$

   with $d = \pm 1$, and $i = mN_{bps} + n$ with $n = 0, \ldots, N_{bps} - 1$.
3. The *a posteriori probability of a data sequence*, i.e.,

$$\lambda(\underline{a}) = P(\underline{a} \,|\, \underline{z}) \tag{26}$$

   with $\underline{a} \in \underline{A}$, and $\underline{A}$ being the set of all possible data sequences.

Deciding in favor of the symbol, bit, or sequence for which the a posteriori probability (*soft value*) is maximum makes hard symbol, bit, or sequence decisions, e.g., $\hat{a}_m = \arg\max_{a \in A} \{\lambda(a_m = a)\}$, $\hat{d}_i = \arg\max_{d \in \{\pm 1\}} \{\lambda(d_i = d)\}$. The a posteriori probability of the data symbol and the data bit are respectively obtained as follows (ignoring a constant factor):

$$\begin{aligned}\lambda(a_m = a) \sim \sum_{(S_{m-1}, S_m) \in T(a)} &(\alpha_{m-1}(S_{m-1}) \\ &\gamma_m(S_m, z_m \mid S_{m-1})\beta_m(S_m))\end{aligned} \tag{27}$$

$$\begin{aligned}\lambda(d_i = d) \sim \sum_{(S_{m-1}, S_m) \in T(d)} &(\alpha_{m-1}(S_{m-1}) \\ &\gamma_m(S_m, z_m \mid S_{m-1})\beta_m(S_m))\end{aligned} \tag{28}$$

where the sum in (27) is computed over all state transitions that are determined by the symbol $a_m = a$, while the sum in (28) is computed over all state transitions that are determined by the bit $d_i = d$. Further, $\alpha_m(S_m)$ and $\beta_{m-1}(S_{m-1})$ are recursively computed as

$$\alpha_m(S_m) = \sum_{S_{m-1} \in \Sigma} \alpha_{m-1}(S_{m-1})\gamma_m(S_m, z_m | S_{m-1}) \tag{29}$$

$$\beta_{m-1}(S_{m-1}) = \sum_{S_m \in \Sigma} \beta_m(S_m)\gamma_m(S_m, z_m \mid S_{m-1}) \tag{30}$$

with Σ being the set of all possible states. The cardinality of such a set, $|\Sigma|$, can be assumed finite with practically time-frequency limited sub-channel impulse responses. We can now summarize the fundamental operations for computing the a posteriori probabilities:

1. Compute the z-parameters (sub-channel matched filters outputs), and s-parameters (sub-channel cross-correlations).
2. Consider a block of matched filter outputs of finite length L that correspond to the finite time window I. Order the matched filter outputs and consequently the data symbols in accordance to the definitions (18), (17). Initialize $\alpha_0(S_0)$ and $\beta_L(S_L)$, setting them to 1 in correspondence to the known starting and ending states and to zero otherwise. Recursively compute $\alpha_m(S_m)$ and $\beta_m(S_m)$ according to (29) and (30).

3. Once $\alpha_{m-1}(S_{m-1})$ and $\beta_m(S_m)$ have been computed, they can be multiplied with the appropriate $\gamma_m(S_m, z_m \mid S_{m-1})$ to obtain $\lambda(a_m)$ or $\lambda(d_i)$ according to (27), (28). The evaluation of the transition probability $\gamma_m(S_m, z_m \mid S_{m-1})$ requires the a priori probability of the symbols/bits that are associated with such a transition, i.e., $P(S_m \mid S_{m-1})$. Clearly, it can be set to a constant value if it is unknown, i.e., bits/symbols are considered equally likely. Assuming independent data bits such an a priori probability can be further factored as follows:

$$P(S_m \mid S_{m-1}) = \prod_{n=0}^{N_{bps}-1} P(d_{mN_{bps}+n}). \qquad (31)$$

The algorithm that we have described is the optimal multicarrier multiuser detector in the probabilistic sense. It delivers soft outputs at bit level, symbol level, and sequence level. Therefore, it is suited for application in concatenated systems with interleavers, e.g., when channel coding with interleaving is deployed. It is based on a coherent metric that requires estimation of the time offset, the frequency offset, and the time-variant impulse response of all sub-channels of all users. If the channel is static, the z-parameters and s-parameters can be calculated off line once for all the transmission duration.

The transition probability that is used in the MAP algorithm includes the a priori information on the transmitted symbols/bits. The estimation of it can be performed iteratively in a coded system by exploiting the redundancy introduced by the channel encoders. The resulting receiver implements a form of turbo detection and decoding [25]. If no a priori information is included in the transition probability, the algorithm delivers the maximum likelihood solution. Such a solution is efficiently obtained with a Viterbi algorithm over the 3-D trellis.

Finally, the implementation of the MAP algorithm requires the utilization of probabilities, and in particular the computation of the channel transition probability through exponential functions. A simplified implementation of the algorithm is possible by operating in the logarithm domain [18]. It is usually referred to as *log-MAP algorithm*.

Digital Implementation of the Front-End Receiver

In FMT-MA systems, the receiver front-end (where the z-s–parameters are computed) can be efficiently implemented via discrete-time processing based on FFT and polyphase low rate filtering. Details can be found in [35]. As an example, let us consider a critically sampled FMT-MA system. Further, let us make the following assumptions: identical time/frequency offsets for all sub-channels of a given user; sampling rate $1/T$; propagation through a tapped delay line channel model with static fading tap gains, i.e., $g_E^u(t) = \sum_{p=-N_p}^{N_p} \alpha^u(p)\delta(t - pT)$; time offset $\Delta t_u = p_u T + \varepsilon_u$, with ε_u being a fraction of T included in the tapped delay line channel model. With these assumptions, the receiver front-end (**Figure 6**) comprises RF demodulation and pre-filtering with a pulse matched to the broadband transmit filter. Then, the following stages are implemented for all users: frequency offset compensation (assuming it to be much smaller than $1/T$) and time offset compensation; weighting (with the conjugate of the channel tap gains) and combining the delayed replicas of the signal at the output of a delay line; S/P conversion and low rate filtering with a pulse matched to the sub-channel filter; M-point FFT. It is interesting to note that this structure resembles a RAKE receiver [29]. In fact, the channel rays are coherently combined and then processed to generate M narrow band sub-channels. In a DMT system, the sub-channel transmit filters are irrelevant, such that in the receiver front-end we do not need to run sub-channel matched filtering.

Sub-Optimal Multicarrier Multiuser Detection

Optimal multicarrier-multiuser detection may be too complex to be practical for a relatively high number of users and sub-carriers. To reduce the complexity of the detection stage, we can pursue an ad hoc design of the system, such as

- Introduce some level of time and frequency synchronization among users. For instance, a control loop from the base station can be deployed such that the terminals can adjust their local oscillators and timing [45].

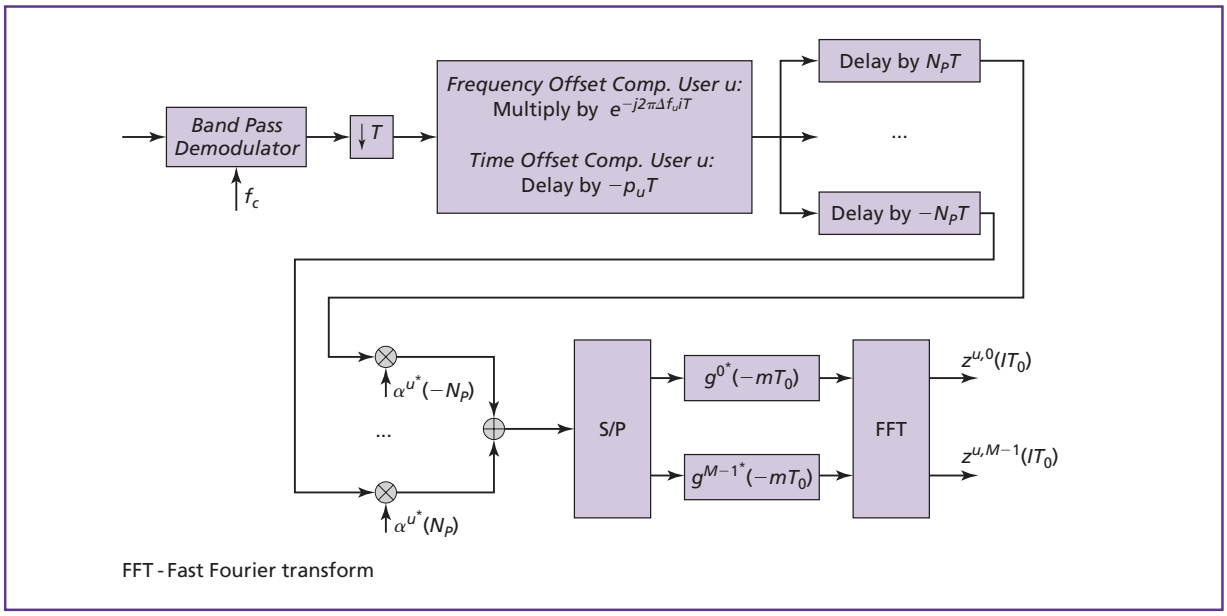

Figure 6.
Discrete-time implementation of the front-end receiver for a critically sampled FMT-MA system with a static tapped delay line channel (portion shown relative to user u).

- Lower the interference components by the appropriate choice of the sub-carrier spacing, the design of the prototype filters, the design of the tone allocation strategy, and the insertion of time and frequency guards. For instance, with time and frequency concentrated pulses, as the Gaussian pulses, the number of interfering sub-channels and the number of ISI terms can be kept small. If the sub-channels have non-overlapping spectra equalization takes place separately on each sub-channel.

We can as well deploy sub-optimal (simplified) detection algorithms. In this paper, we focus on simplified methods that are based on reducing the complexity of the MAP algorithm. We first describe methods to reduce the number of states in the MAP algorithm. Then, we describe simplified MAP detection based on iterative detection on sub-trellises. It should be noted that other sub-optimal detection approaches could be borrowed from the CDMA literature [29]. For instance, we could appropriately define, for application to a MC-MA system, the decorrelating detector and the minimum mean square error (MMSE) detector.

Reduced-State MAP Multicarrier Detection

Let us consider the full state 3-D trellis with all possible transitions. Reducing the number of states implies that some of the branches in the full state 3-D trellis are cut. This is done dynamically as we move through the 3-D trellis by retaining only a certain amount of states. This is equivalent to forcing hard decisions on some of the past (in the user-frequency-time sense) transmitted data symbols. It should be noted that the BCJR algorithm requires a forward and backward recursion on a full 3-D trellis. Nevertheless, it is possible to reduce the number of states by retaining, for instance, the forward direction reduced trellis also for the backward direction.

Since three dimensions are involved, more freedom is left on how to choose the surviving states. We can, for instance, extend the M-algorithm [3] or the decision-feedback algorithm [17] to the context that we are considering here. It is straightforward to extend the M-algorithm, by just retaining at each step the states with the best metric (highest probability). With decision feedback, we force hard decisions as we proceed onto the 3-D trellis, such that at each step only a few states/paths are retained. For instance, we

can reduce the 3-D trellis into a 2-D trellis by decision feedback in either the user, or the temporal, or the frequency dimension. Another way to proceed is to retain a 3-D trellis but reduce, through decision feedback, the memory in each dimension. In other words, we can keep a lower amount of states on each dimension.

Iterative Sub-Trellis Detection

Instead of implementing the full state optimum detector, we can approach the MAP solution by partitioning the full 3-D trellis into independent subtrellises. Decisions made on each trellis can be exchanged among the trellises (**Figures 7**, **8**, and **9**). Exchange of information can be done in parallel or in serial mode.

If channel coding is deployed, the detectors and the decoders can be concatenated in a parallel or serial fashion depending on how channel coding is done (see next section). To limit error propagation, it may be beneficial to use soft symbol decisions whenever reliability information is available (for instance, at the output of the soft output channel decoders). Soft decision feedback can be directly included in metric (20) by using instead of the hard symbols a_m their average value, i.e., $\overline{a}_m = \sum_{a \in A} aP[a_m = a]$.

Special cases of iterative sub-trellis detection are per-user, per-carrier, and per-symbol detection.

Iterative Per-User Detection

Per-user detection is accomplished when splitting the 3-D trellis into a bank of N_U 2-D trellises. Each detector performs equalization in time and frequency for a given user and takes into account the information on the MAI by feedback from the other detectors (Figure 7). If the 2-D trellises are concatenated in parallel, the data decisions are reused in a new parallel detection stage after detection from all trellises is completed. If they are serially concatenated, a given user detector can immediately use the decisions provided by the previous user detector. The similarity to parallel and serial interference cancellation in CDMA systems is clear [27, 48]. Note that this approach basically consists on canceling the interfering terms using soft/hard decisions from other independent detection stages. Typically, cancellation is done in three steps: make decisions on the transmitted symbols, regenerate the individual received signals, and subtract

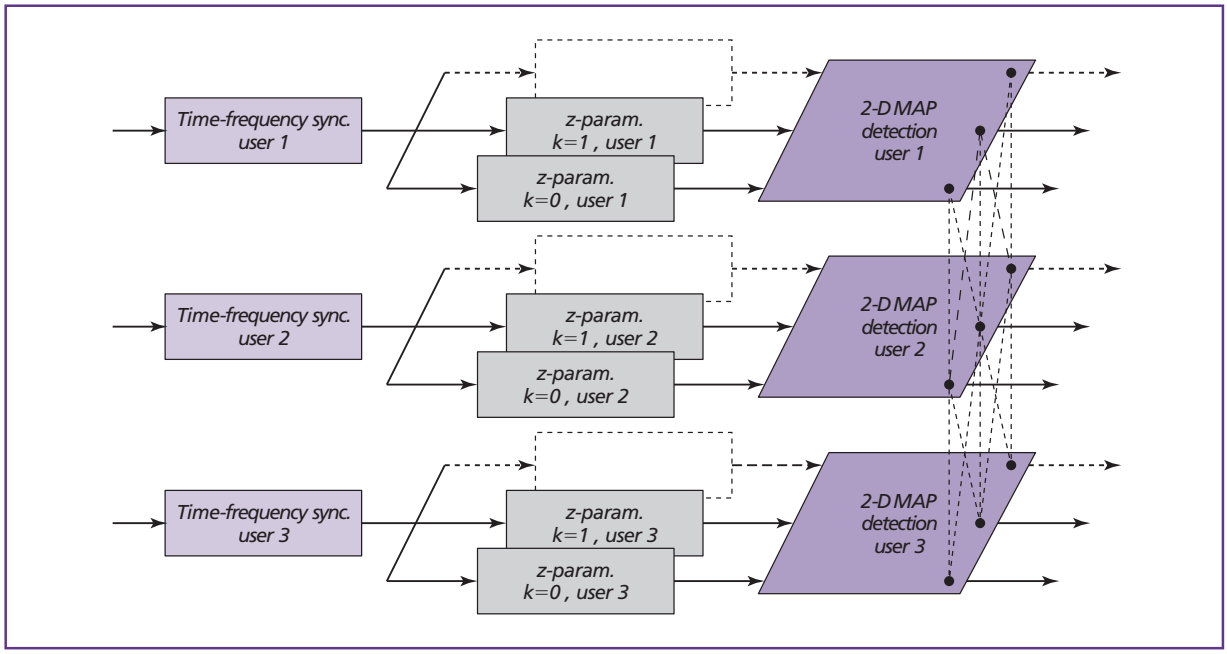

Figure 7.
Iterative per-user detection (with exchange of information taking place in the user direction).

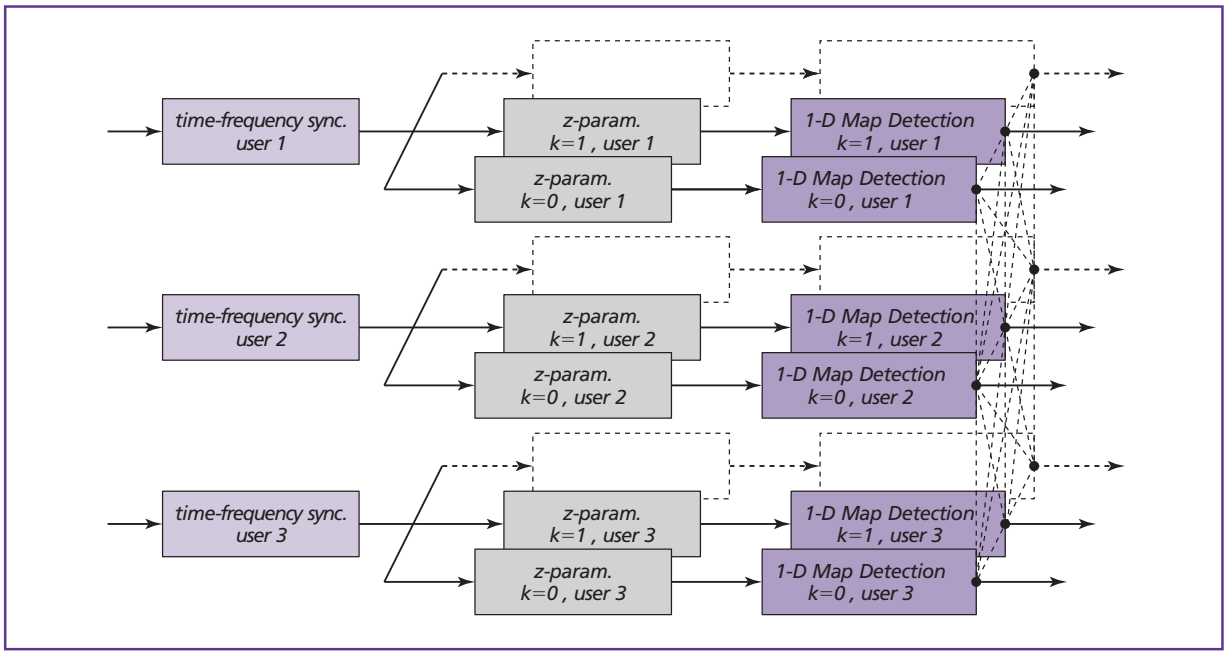

Figure 8.
Iterative per-carrier detection (with exchange of information taking place in the frequency and user direction).

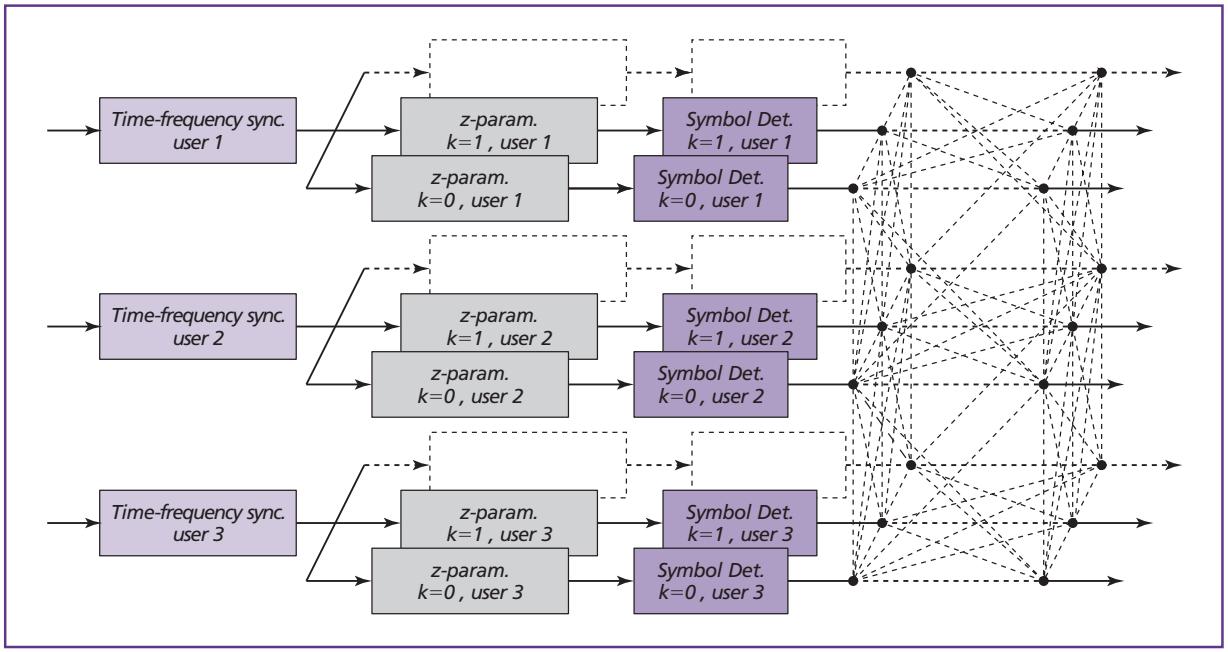

Figure 9.
Iterative per-symbol detection (with exchange of information taking place in the temporal, frequency, and user direction).

them from the original received signal. However, regeneration is not necessary since decisions can be directly included in the metric (20).

Iterative Per-Carrier Detection

A further reduction in complexity is obtained by splitting the 3-D trellis into a bank of MN_U single-carrier detectors (assuming, in principle, that all users can deploy all available sub-carriers). Each detector is single carrier based, meaning that it just performs equalization in the temporal direction separately for each sub-carrier (Figure 8). Again exchanging of information can be done in a parallel or in a serial iterative mode.

Iterative Per-Symbol Detection

A more drastic reduction in complexity is achieved by making symbol-by-symbol decisions. That is, we make decisions on the transmitted data symbols by processing a single matched filter output at the time. The symbol-by-symbol detectors can still be iteratively concatenated. Once we have made soft/hard decisions on a given data symbol (of a given user and sub-carrier), it can be included in the metric that is used for the detection of a new symbol (Figure 9). For instance, parallel *iterative per-symbol detection* can be implemented as follows:

- At the first pass, make hard decisions on all data symbols of a given transmission block, i.e., compute for all $u = 1, \ldots, N_U$, $k = 0, \ldots, M-1$, $lT_0 \in I$:

$$\hat{a}^{u,k}(lT_0)_{it=0} = \arg\max_{a\in A}\{\mathrm{Re}\{a^*(2z^{u,k}(lT_0) - as^{u,u,k,k}(lT_0, lT_0))\}\}. \quad (32)$$

- Run a new per-symbol detection stage including the available decisions from the previous iteration, i.e., compute for all $u = 1, \ldots, N_U$, $k = 0, \ldots, M-1$, $lT_0 \in I$:

$$\hat{a}^{u,k}(lT_0)_{it=i} = \arg\max_{a\in A}\left\{\mathrm{Re}\left\{a^*\left(2z^{u,k}(lT_0) - as^{u,u,k,k}(lT_0, lT_0) - \sum_{(u',k',l')\neq(u,k,l)} 2\hat{a}^{u',k'}(l'T_0)_{it=i-1}s^{u,u',k,k'}(lT_0, l'T_0)\right)\right\}\right\}. \quad (33)$$

The sum is computed over all possible terns (u', k', l') that differ from the tern (u, k, l).

The decision metric above is obtained by isolating in (A-3) and (A-4) of the Appendix, the terms that depend upon the data symbol that we are detecting. Note that the metric requires knowledge of the s-parameters that in practice have to be estimated.

Clearly, detection can take place in serial mode by including in the metric the data decisions as soon as they come available. It can also be advantageous to start detection from the user/carrier that has the best signal power. That is, we run a sort of ordered (according to the power level) detection process. Further, soft data decisions $\bar{a}^{u',k'}(l'T_0)$ (instead of hard data decisions $\hat{a}^{u',k'}(l'T_0)$) can be included in the metric.

Coded Multicarrier Multiple Access

The channel coding problem in a MC-MA system is fundamentally a problem of coding for MIMO channels. We see a similarity to the space-time coding problem in multiple antenna systems [32, 33, 36, 38]. However, coding in multicarrier systems takes place in the frequency–time domain while coding in multiple transmit antenna systems takes place in the space–time domain. That is, the sub-channels in space–time-coded systems entirely overlap in frequency while the sub-channels in a multicarrier system have a degree of overlapping that depends upon the design of the sub-carrier spacing and the transmit filters shape. From a diversity point of view, the resource to be exploited in a space–time-coded system is the spatial diversity of rich scattering environments, while in multicarrier systems is the frequency diversity of frequency-selective fading channels. Clearly, a combination of space–time coding and multicarrier modulation is possible.

In this paper, we propose the deployment of bit-interleaved codes [9] and describe decoding based on the iterative (turbo) concatenation of the multicarrier-user detector and the channel decoders. It should be noted that the proposed detector is an optimum soft-in soft-out module. That is, it provides the a posteriori probabilities of the data bits/symbols transmitted by all users and accepts the corresponding a priori probabilities.

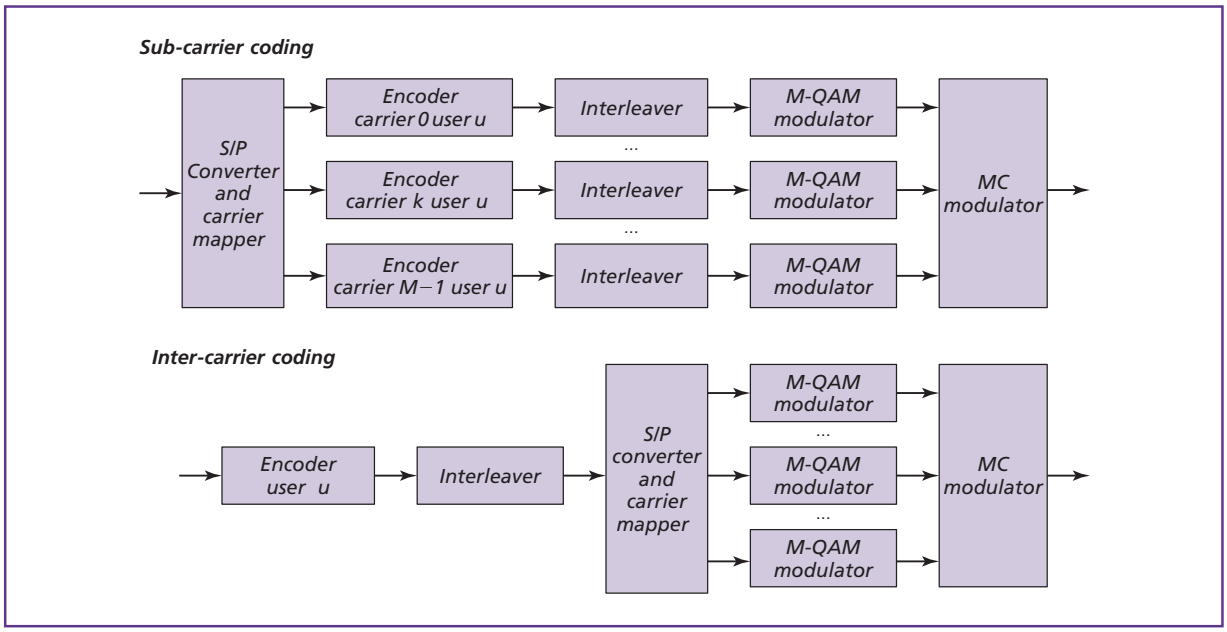

Figure 10.
Sub-carrier and inter-carrier channel coding for user u.

Two forms of coding are possible. In *sub-carrier interleaved coding*, distinct information bits streams are transmitted over distinct sub-carriers and are independently encoded (**Figure 10**). In other words, each stream is encoded, interleaved, and mapped to complex data symbols. Finally, the parallel symbol streams are multicarrier modulated. In *inter-carrier interleaved coding* (Figure 10), the original information bit stream is encoded and interleaved. Then, the encoded bit stream is parsed into a number of sub-streams equal to the number of assigned sub-carriers. Each sub-stream of bits is mapped into complex data symbols. Finally, multicarrier modulation takes place.

Turbo Multicarrier-User Decoding

When interleaved codes are deployed, optimal maximum likelihood decoding requires jointly taking into account the structure of the encoder, the interleaver, the modulator, and the channel. Practical and simplified decoding is accomplished through the turbo decoding approach by treating the system as a concatenated coded system [18]. Essentially, we run multicarrier-user detection; then after de-interleaving we run channel decoding (**Figure 11**). Further, we can iteratively concatenate demodulation and decoding by passing feedback information from the decoders. The multicarrier-user detector has now to provide the a posteriori probabilities of the coded bits, which are then de-interleaved and passed to the decoders. The decoders can be implemented with a soft-in soft-out algorithm, e.g., MAP decoder for convolutional codes [5], and are capable to deliver new a posteriori probabilities of the coded bits. These are interleaved and passed back to the multicarrier detector where they are used as an estimate of the a priori transition probabilities [see 31]. To minimize the correlation with previously computed soft information, extrinsic information has to be exchanged [18, 36].

The turbo decoding approach has found many applications since it was deployed for decoding of turbo codes [7]. It has been proposed for turbo equalization of coded 2-PSK signals in [14], for turbo decoding of differentially encoded M-PSK signals in [34], and for turbo multiuser decoding of coded CDMA signals in [25]. Recently, it has been investigated as an effective technique in coded space-time architectures with multiple antennas [4, 33, 36, 38].

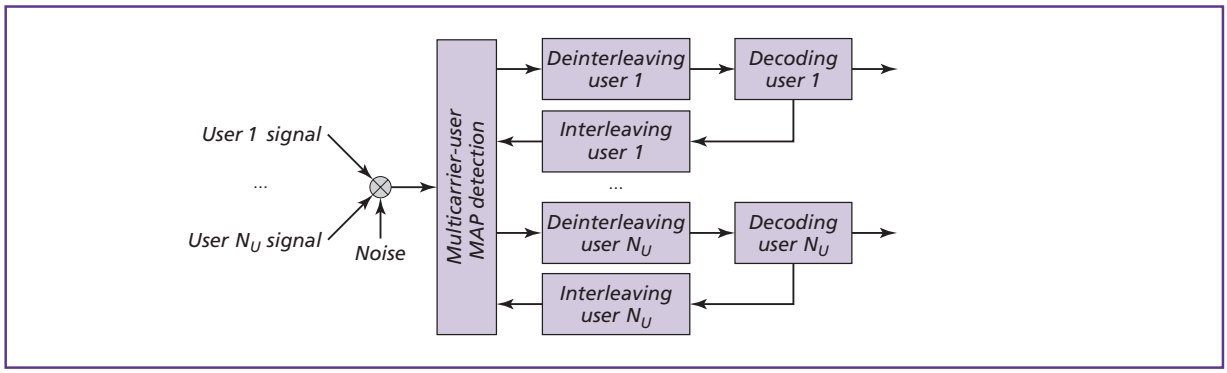

Figure 11.
Turbo multicarrier-multiuser decoding.

Simplified turbo multicarrier-user decoding can be implemented by concatenating simplified detectors with simplified decoders. For instance, we can use the simplified detection methods that we have previously described. Further, we can pass hard feedback information, which requires conventional hard output decoders.

A drastic simplification is obtained by using a simple per-symbol based detector. At the first detection stage, we generate soft outputs by neglecting the presence of the interference components. Then, we apply channel decoding and we feed back soft or hard information on the data symbols of all users. Now we can re-run detection including in the metric calculation the soft/hard knowledge of all interfering data symbols. We refer to this approach as *iterative per-symbol decoding*. The computation of the logarithm of the a posteriori probability of a given coded bit (transmitted by user u on sub-carrier k) can be simplified at the detection stage as follows:

$$\ln \lambda(d_m = d)_{it=i} \sim \max_{a \in A(d_m=d)} \{\mathrm{Re}\{a^*(2z^{u,k}(lT_0) - as^{u,u,k,k,}(lT_0, lT_0) - \sum_{(u',k',l') \neq (u,k,l)} 2\hat{a}^{u',k'}(l'T_0)_{it=i-1} s^{u,u',k,k'}(lT_0, l'T_0))\}\}, \quad (34)$$

where $\hat{a}^{u,k}(lT_0)_{it=i-1}$ are the soft/hard data symbols provided by the channel decoders at the previous iteration. At the first detection pass they are set to zero. $A(d_m = d)$ is the set of data symbols $a^{u,k}(lT_0)$ (of user u, sub-carrier k, instant lT_0) that are labeled with bit $d_m = d$. Such a set has cardinality $2^{N_{bps}-1}$ with N_{bps} number of bits per data symbol. The above result is obtained by approximating the logarithm of the sum of exponentials, with the exponent that has the largest value.

Performance Evaluation

To illustrate the main advantages and potentiality of the proposed multicarrier-user detection approach, we report performance curves that have been obtained by computer simulations. We consider several FMT/DMT system scenarios to show the effect of the time and carrier frequency offsets across users, the effect of static and time-variant fading, and of the channel frequency selectivity. We consider the deployment of rectangular pulses (DMT) and Gaussian pulses (FMT). We report bit-error-rate (BER) versus signal-to-noise ratio (SNR per symbol) curves to compare the performance of optimal multicarrier-multiuser detection (full complexity), iterative per-symbol detection/decoding (labeled in the figures with PSD and the associated iteration number), and conventional detection of DMT. In particular for the former we report performance bounds (labeled in the figures with BOUND) that correspond to the performance achieved with ideal multicarrier-user detection, i.e., with perfect knowledge of all interfering data symbols and perfect interference cancellation. These bounds correspond to the matched filter performance bounds [37, 44]. When channel coding is deployed (according to the inter-carrier coding

scheme of Figure 10), the bounds are obtained by running ideal multicarrier detection followed by channel decoding. Iterative per-symbol detection/decoding is implemented according to (32)–(34). The results show that iterative per-symbol detection with a small number of iterations can perform close to ideal multicarrier detection.

Scenario A: Asynchronous Multiuser System in AWGN

In this scenario, we assume to multiplex $N_U = 2$ or $N_U = 4$ users in a MT-MA system with $M = 16$ uniformly spaced sub-carriers. The system is critically sampled, i.e., $N = M$, $F_0 = 1/T_0 = 1/T_1$. The users deploy M/N_U distinct sub-carriers each. The tones have equal power and are allocated across users with either an interleaved (**Figure 12**) or a block scheme (**Figure 13**). Both rectangular in time prototype filters with no cyclic prefix (DMT-MA), and Gaussian-shaped filters with $f_{3dB}T_0 = 0.33$ (FMT-MA) are considered. The users are asynchronous, and they experience a time misalignment that is uniformly distributed between $[-\Delta t_{max}, \Delta t_{max}]$, and a frequency offset that is uniformly distributed between $[-\Delta f_{max}, \Delta f_{max}]$, relatively to a fixed reference point at the receiver. The time/frequency offsets are statistically independent across distinct users, but they are assumed to be identical for all sub-channels of a given user. Propagation is through an AWGN channel with no fading.

In Figures 12 and 13, the solid curves correspond to the performance without channel coding while the dotted curves to the performance with channel coding. In the uncoded case, each user transmits a frame of $320/N_U$ information bits that are mapped to 4-PSK symbols. These frames of information symbols correspond to 10 DMT/FMT symbols over which the time/frequency offset is constant, and changes randomly over the next 10 DMT/FMT symbols. In the coded case the users are independently coded and transmit frames of $160/N_U$ information bits that are encoded with a rate 1/2 convolutional code with memory 2. The resulting $320/N_U$ coded bits are randomly interleaved, mapped to 4-PSK symbols according to the Gray rule, and assigned to the sub-carriers (as shown in the inter-carrier coding scheme of Figure 10).

The bound curves correspond to the BER performance of ideal multiuser detection, i.e., when detection takes place with perfect interference cancellation. The other curves (labeled with PSD and the associated iteration number) correspond to the BER performance of iterative per-symbol detection/decoding. Decision feedback is hard, which requires conventional hard output Viterbi decoders in the case of coded transmission [see (34)]. Up to 6 and up to 2 iterations are considered, respectively, in the uncoded case and the coded case. In general, PSD at the first iteration (when according to (32) the interference components are neglected) exhibits a significant error floor as a result of the high MAI. The error floor diminishes with the deployment of the block tone multiplexing compared to the interleaved tone multiplexing since less MAI is introduced. Channel coding allows for error correction yielding lower error floors. We emphasize that the curves are plotted assuming the SNR per transmitted symbol and not the SNR per transmitted bit.

A significant performance improvement is found with few PSD iterations. Looking at Figure 12, per-symbol detection of uncoded FMT outperforms uncoded DMT at the 6-th iteration and comes close to the performance of ideal multiuser detection (error rate bound). With channel coding and two PSD iterations the advantage of FMT over DMT is less pronounced. If we now observe Figure 13, we can see that, with the block tone multiplexing, PSD of uncoded DMT exhibits lower error floors. With coding and block multiplexing, iterative per-symbol decoding of DMT yields performance almost identical to the bound with only two iterations.

These results illustrate that iterative per-symbol detection/decoding can yield performance results that are near to the error rate with ideal multiuser detection.

Scenario B: Asynchronous Multiuser System in Rayleigh Fading

We now consider the coded (with a bit-interleaved convolutional code of rate 1/2 and memory 2) multiuser system of scenario A when transmission is through a Rayleigh fading channel (**Figure 14**). The fading is assumed to be static over the duration of a frame. Both flat fading and 2-rays fading with independent equal power rays are considered. The second

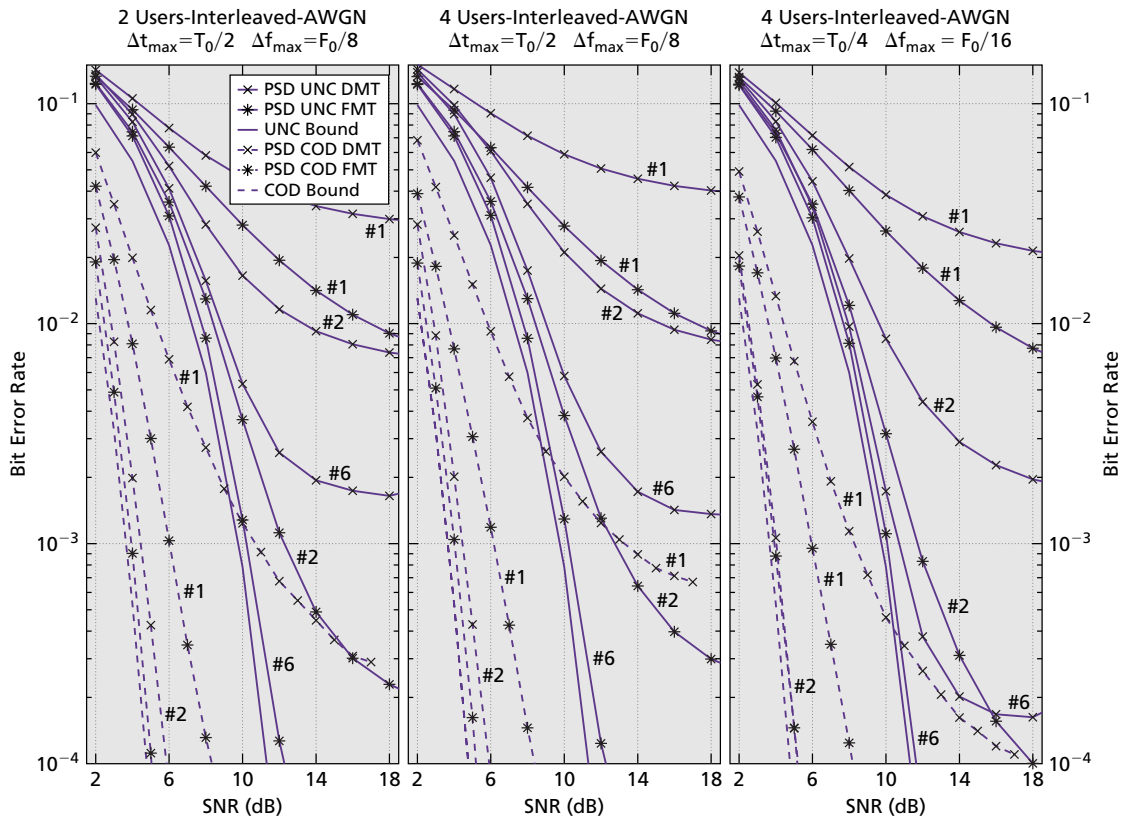

AWGN - Additive white Gaussian noise
BOUND - Ideal multicarrier detection and decoding
COD - Coded system with rate 1/2 convolutional code and bit-interleaving
DMT - Discrete multitone modulation (rectangular filters)
FMT - Filtered multitone modulation (Gaussian filters)
PSD - Iterative per-symbol detection (up to 6 iterations) and decoding (up to 2 iterations).
SNR - Signal-to-noise ratio
UNC - Uncoded system

2- and 4-user systems with 16 total carriers and 4-PSK modulation. Interleaved tone multiplexing. AWGN channel with asynchronous users. Users' time offsets and frequency offsets independent and uniformly distributed respectively in $[-\Delta t_{max}, \Delta t_{max}]$ and in $[-\Delta f_{max}, \Delta f_{max}]$.

Figure 12.
Average BER performance of uncoded and convolutionally coded critically sampled MT-MA with Gaussian filters (FMT) and rectangular (DMT) in AWGN.

ray is delayed by $\delta = T$ or $\delta = 2T$. The users are asynchronous with uniformly distributed time/frequency offsets. In the 2-users system (left-most and center plot), only the performance of the block multiplexing scheme is shown. In the 4-users system (right-most plot) the performance of both the block and the interleaved multiplexing schemes is shown.

In general the effect of fading is to yield worse BER performance than in AWGN. However, with only two or three iterations the performance of PSD is very close to the performance bound (ideal multicarrier detection). In flat fading (left-most plot of Figure 14), DMT (rectangular filters with no guard time) and FMT (Gaussian filters with $f_{3dB}T_0 = 0.33$) have almost

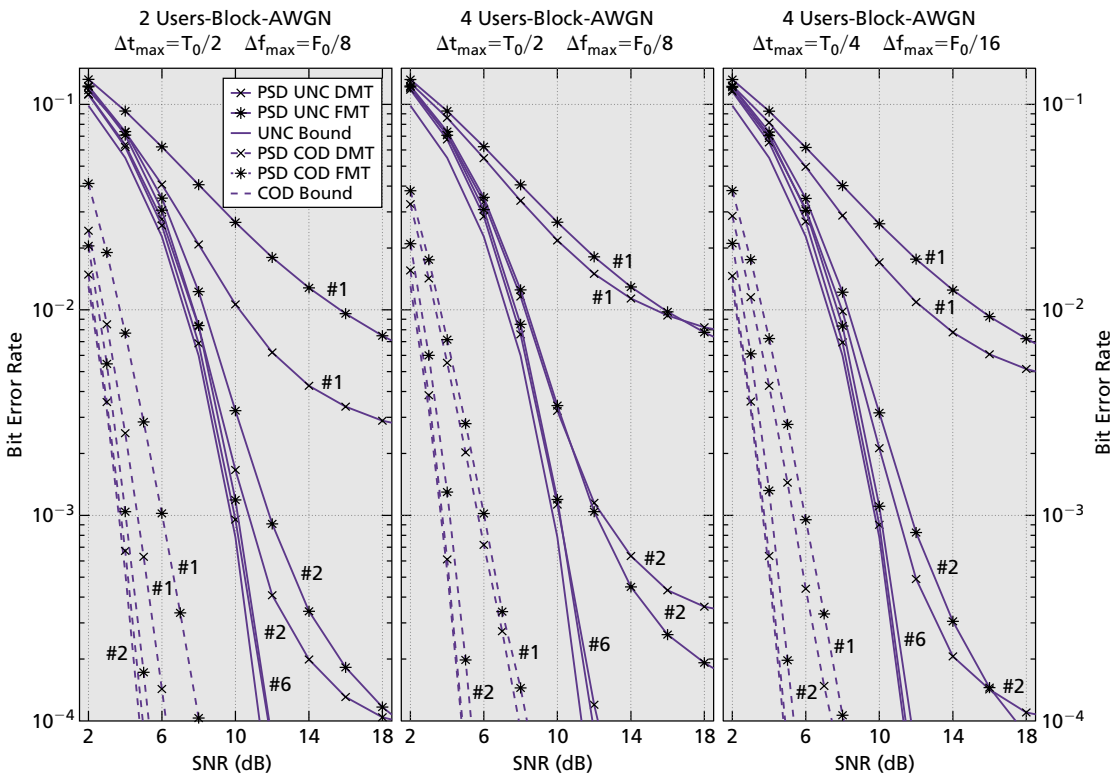

AWGN - Additive white Gaussian noise
BOUND - Ideal multicarrier detection and decoding
COD - Coded system with rate ½ convolutional code and bit-interleaving
DMT - Discrete multitone modulation (rectangular filters)
FMT - Filtered multitone modulation (Gaussian filters)
PSD - Iterative per-symbol detection (up to 6 iterations) and decoding (up to 2 iterations).
SNR - Signal-to-noise ratio
UNC - Uncoded system

2- and 4-user systems with 16 total carriers and 4-PSK modulation. Block tone multiplexing. AWGN channel with asynchronous users. Users' time offsets and frequency offsets independent and uniformly distributed respectively in $[-\Delta t_{max}, \Delta t_{max}]$ and in $[-\Delta f_{max}, \Delta f_{max}]$.

Figure 13.
Average BER performance of uncoded and convolutionally coded critically sampled MT-MA with Gaussian filters and rectangular filters (DMT) in AWGN.

identical performance bounds. In the 2-users system with 2-rays fading (center plot), DMT yields a better performance bound than FMT. Further, the channel frequency selectivity provides frequency diversity such that the performance is improved over the flat fading case. In the 4-users system over a 2-ray channel (right-most plot), we consider only coded FMT and show that with the interleaved tone multiplexing it is possible to obtain better performance than with the block tone multiplexing.

Scenario C: DMT, FMT, and DMT with Cyclic Prefix in Rayleigh Fading

In **Figure 15**, we report the performance of a single-user system that deploys 8 sub-carriers and 4-PSK modulation with or without channel coding. In

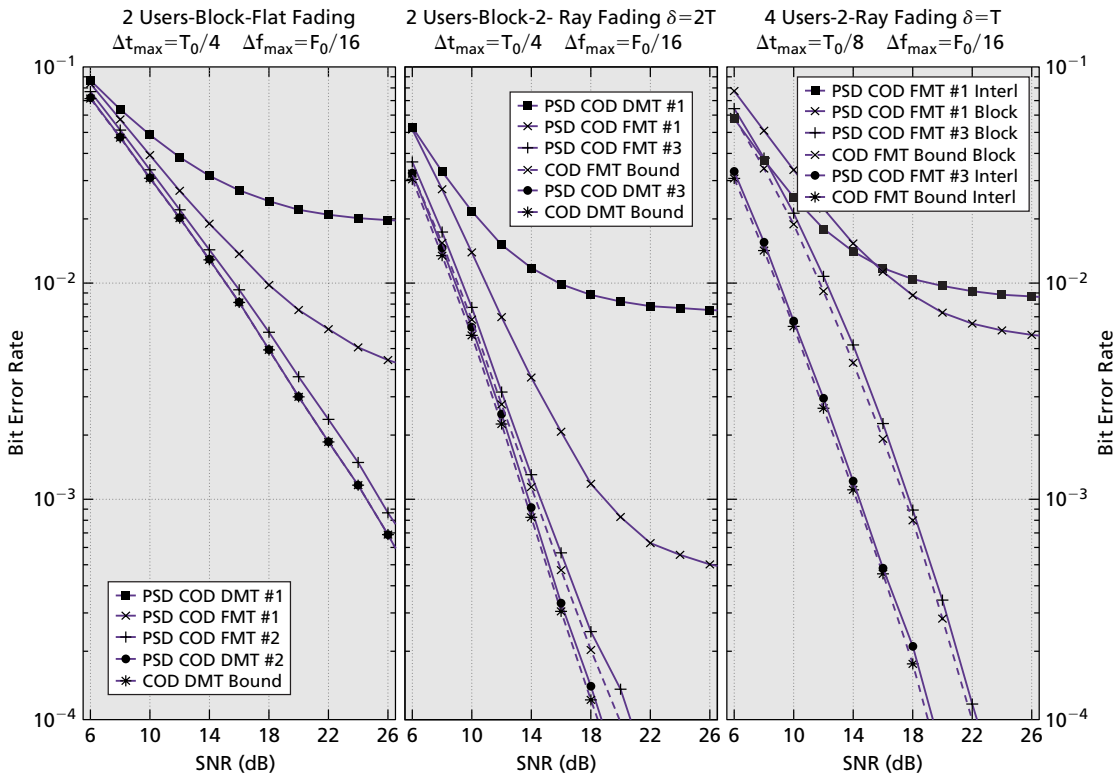

BOUND - Ideal multicarrier detection and decoding
COD - Coded system with rate ½ convolutional code and bit-interleaving
DMT - Discrete multitone modulation (rectangular filters)
FMT - Filtered multitone modulation (Gaussian filters)
PSD - Iterative per-symbol detection and decoding (up to 3 iterations).
SNR - Signal-to-noise ratio

2- and 4-user systems with 16 total carriers and 4-PSK modulation. Block and interleaved tone multiplexing. Rayleigh fading channel and asynchronous users. Users' time offsets and frequency offsets independent and uniformly distributed respectively in $[-\Delta t_{max}, \Delta t_{max}]$ and in $[-\Delta f_{max}, \Delta f_{max}]$.

Figure 14.
Average BER performance of convolutionally coded critically sampled MT-MA with Gaussian filters (FMT) and rectangular filters (DMT). Rayleigh fading channel and asynchronous users.

the former case, a rate 1/2 memory 2 convolutional code with random-bit interleaving is used before DMT/FMT modulation. We want to investigate the effect of the prototype pulse when propagation is through a fading channel, and in particular: (a) flat Rayleigh fading that is static for the MT block duration; (b) fast Rayleigh fading according to the Jakes' model, i.e., time variant over the MT block duration with a normalized Doppler spread f_dT = 0.01, 0.1; (c) 2-rays channel with independent and Rayleigh faded rays that are static for the MT block duration; the second ray is delayed by $3T$.

We show performance curves for conventional detection of DMT, iterative per-symbol decoding of DMT, and ideal multicarrier detection (performance bound with perfect cancellation of all interfering data symbols) for both DMT and FMT. In the left-most plot of Figure 15, we consider flat fading. The performance bounds show that with ideal detection of MT modulation, we can exploit the time diversity provided by

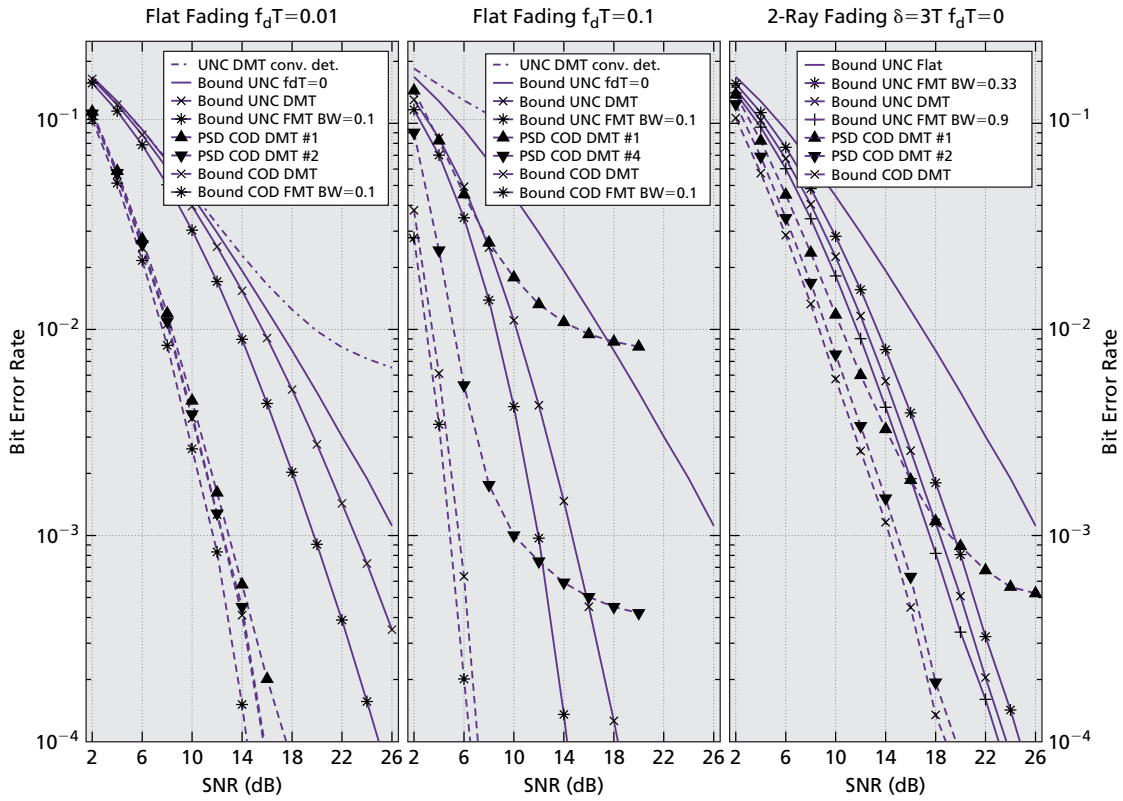

BOUND - Ideal multicarrier detection and decoding
BW - Normalized bandwidth of Gaussian filter
COD - Coded system with rate 1/2 convolutional code and bit-interleaving
DMT - Discrete multitone modulation (rectangular filters)
FMT - Filtered multitone modulation (Gaussian filters)
PSD - Iterative per-symbol detection/decoding (up to 4 iterations)
SNR - Signal-to-noise ratio
UNC - Uncoded system

One user with 8 sub-carriers and 4-PSK modulation. Left-most plot, flat Rayleigh fading (time-variant) with normalized Doppler $f_dT = 0.01$. Center plot, flat Rayleigh fading with normalized Doppler $f_dT = 0.1$. Right-most plot, 2-rays Rayleigh fading with second ray delayed by 3T.

Figure 15.
Average BER performance of critically sampled MT modulation (one user) with Gaussian filters (FMT) and rectangular filters (DMT) in Rayleigh fading.

time-variant fading. Note that significant improvements are found over the static fading curve. Further, conventional detection of DMT does not cope with the intercarrier interference introduced by fast fading and exhibits an error floor. FMT with Gaussian filters and normalized bandwidth $f_{3dB}T_0 = 0.1$ has a better performance bound than DMT in both the uncoded and the coded case. With iterative PSD of coded DMT and only two iterations, we approach the associated performance bound. Although not shown, when the normalized bandwidth of the Gaussian filter is 0.33 the performance is similar to DMT. If the normalized Doppler increases to 0.1 (center plot), the performance of ideal multicarrier detection improves due to increased time diversity, while conventional detection of DMT exhibits a very high error floor. Even at these

extreme channel conditions, iterative PSD of coded DMT significantly lowers the error rate floor.

In the right-most plot of Figure 15, we consider a 2-rays static fading channel. The figure shows that ideal multicarrier detection of uncoded DMT (without cyclic prefix) exploits the channel frequency diversity and yields better performance than in flat fading. It should be noted that conventional detection of uncoded DMT with cyclic prefix is identical in both flat and frequency-selective fading, i.e., it does not provide frequency diversity gains. Further, the redundancy of the cyclic prefix introduces a signal-to-noise ratio penalty. The results show also that the error rate bound of FMT with Gaussian filters and normalized bandwidth 0.33 is worse than DMT. However, if we increase the normalized bandwidth to 0.9, we can get better performance than DMT. Finally, in this figure we report the performance of iterative PSD of coded DMT (without cyclic prefix) and we show that with only two iterations the performance is close to the bound.

The main conclusion here is that, with optimal multicarrier detection, we can exploit both the temporal and the frequency diversity. The diversity gains are a function of the sub-channel filter. Narrowing the bandwidth of the sub-channel filters can provide higher time diversity gains, while spreading the bandwidth of the sub-channel filters can provide higher frequency diversity gains [37].

Concluding Remarks

In this paper, we have considered multicarrier-multiuser architectures and their deployment in a multiple-access asynchronous wireless channel. The system design parameters comprise the choice of the sub-channel transmit filters, the sub-carrier spacing, and the tone allocation strategy. The channel temporal and frequency selectivity, as well as the presence of temporal and carrier frequency misalignments across users, causes ICI, ISI, and MAI components at the outputs of the receiver filter bank. Conventional single-user detection can be inadequate to grant reliable communications in broadband applications with high coverage and mobility requirements where the impact of the time and frequency offsets is severe.

With single-user detection, a high degree of synchronization among users is needed, which in turn requires a feedback control from the central receiver whose practicality and reliability has to be investigated. The deployment of time- and frequency-concentrated sub-channel filters and the appropriate allocation of sub-carriers among users help to yield robustness against the users' asynchronism. Lower MAI is generated when the tones are allocated to users in disjoint blocks. Inserting frequency guards between adjacent blocks of tones can further separate the spectrum of distinct users. The use of time-limited pulses (DMT, OFDM) is a very popular choice. When deployed with the insertion of a guard time (cyclic prefix), conventional single-user detection can yield acceptable performance since immunity to the channel time dispersion and users' time misalignment is achieved. However, the carrier frequency offsets still introduce inter-carrier interference and the guard time translates into a loss of spectral efficiency. The deployment of frequency-limited pulses translates into the absence of ICI from both channel time dispersion and users' time misalignment at the expense of small ISI. In this case, only sub-channel equalization is required if the intercarrier interference generated by the frequency offsets is controlled with the insertion of frequency guards. Practically, time- and frequency- limited pulses have to be deployed in order to control both the ISI and ICI components. In this respect, we have found that Gaussian pulses are a reasonable choice.

Despite of what the sub-channel pulse shape is, we have looked into the problem of deriving the optimal maximum a posteriori demodulator in an asynchronous multicarrier multiple-access channel. The optimal demodulator implements the MAP algorithm using an appropriate metric. It is capable of coping with time/frequency asynchronism and time-variant frequency-selective channels. The algorithm is optimal for demodulation of both FMT and DMT signals and is capable of exploiting both the temporal and frequency channel diversity. It is interesting to note that multicarrier modulation can be interpreted as a diversity transform for fading channels that yields diversity and coding gains when optimally demodulated [37].

The optimal demodulation algorithm essentially runs multiuser detection and time/frequency equalization. In general, its complexity grows exponentially with the number of users and sub-channels. Its complexity can be reduced through the deployment of time and frequency concentrated sub-channel pulses in conjunction with reduced state detection techniques. We have found that detection can be simplified by using iterative detection based on exchanging information across sub-trellises. If channel coding is deployed, exchanging of information can be done using soft/hard decisions from the decoders, thus implementing a form of turbo detection and decoding. Iterative per-symbol detection/decoding turns out to be a very simple detection/decoding approach that is capable of yielding performance close to optimal detection.

Finally, we point out that, from a practical implementation standpoint, channel estimation as well as time/frequency offset estimation algorithms have to be studied. The channel estimation task as well as the complexity of the detector can be more challenging in fast time-variant channels. However, the appropriate choice of the sub-carrier spacing allows trading off between the requirement of flat sub-channel frequency response and static channel over the duration of a multitone data block.

Appendix. Metric Derivation

We herein derive the metric in (8), and (19)–(20). Let

$$Z(t) = \sum_{u=1}^{N_U}\sum_{k=0}^{M-1}\left(e^{j(2\pi\Delta f_{u,k}t+\Delta\phi_{u,k})}\sum_{l=-\infty}^{\infty}(\hat{a}^{u,k}(lT_0)e^{j2\pi f_k lT_0} \times g_R^{u,k}(t-\Delta t_{u,k}-lT_0;\, t))\right); \quad \text{(A-1)}$$

then the channel log-likelihood function is decomposed as follows (* denotes complex conjugate):

$$\begin{aligned}\Omega(\underline{\hat{a}}) &= \int_I |y(t)-Z(t)|^2\,dt \\ &= \int_I |y(t)|^2\,dt - 2\mathrm{Re}\left\{\int_I Z(t)^* y(t)\,dt\right\} \\ &\quad + \int_I Z(t)^* Z(t)\,dt \\ &= A + B + C. \end{aligned} \quad \text{(A-2)}$$

The terms A, B, C are defined as follows:

$$\begin{aligned} A &= \int_I |y(t)|^2\,dt, \\ B &= -2\mathrm{Re}\left\{\sum_{lT_0\in I}\sum_{u=1}^{N_U}\sum_{k=0}^{M-1}\hat{a}^{u,k}(lT_0)^* z^{u,k}(lT_0)\right\} \end{aligned} \quad \text{(A-3)}$$

with $z^{u,k}(lT_0)$ defined in (9),

$$C = \sum_{lT_0,l'T_0\in I}\sum_{u,u'=1}^{N_U}\sum_{k,k'=0}^{M-1}\hat{a}^{u,k}(lT_0)^*\hat{a}^{u',k'}(l'T_0)s^{u,u',k,k'}(lT_0,\, l'T_0) \quad \text{(A-4)}$$

with $s^{u,u',k,k'}(lT_0,\, l'T_0)$ defined in (10). We can further partition C as follows:

$$\begin{aligned} C &= \sum_{lT_0\in I}\sum_{u,u'=1}^{N_U}\sum_{k,k'=0}^{M-1}\hat{a}^{u,k}(lT_0)^*\hat{a}^{u',k'}(lT_0)s^{u,u',k,k'}(lT_0,\, lT_0) \\ &\quad + \sum_{lT_0\in I}\sum_{u,u'=1}^{N_U}\sum_{k,k'=0}^{M-1}\sum_{l'<l}\hat{a}^{u,k}(lT_0)^*\hat{a}^{u',k'}(l'T_0)s^{u,u',k,k'}(lT_0,\, l'T_0) \\ &\quad + \sum_{lT_0\in I}\sum_{u,u'=1}^{N_U}\sum_{k,k'=0}^{M-1}\sum_{l'<l}\hat{a}^{u,k}(l'T_0)^*\hat{a}^{u',k'}(lT_0)s^{u,u',k,k'}(l'T_0,\, lT_0). \end{aligned} \quad \text{(A-5)}$$

If we exchange u with u' and k with k' in the last term in (A-5), since $s^{u,u',k,k'}(lT_0,\, l'T_0) = s^{u',u,k',k}(l'T_0,\, lT_0)^*$, C becomes

$$\begin{aligned} C &= \sum_{lT_0\in I}\sum_{u,u'=1}^{N_U}\sum_{k,k'=0}^{M-1}\hat{a}^{u,k}(lT_0)^*\hat{a}^{u',k'}(lT_0)s^{u,u',k,k'}(lT_0,\, lT_0) \\ &\quad + 2\mathrm{Re}\left\{\sum_{lT_0\in I}\sum_{u,u'=1}^{N_U}\sum_{k,k'=0}^{M-1}\sum_{l'<l}(\hat{a}^{u,k}(lT_0)^*\hat{a}^{u',k'}(l'T_0) \times s^{u,u',k,k'}(lT_0,\, l'T_0))\right\}. \end{aligned} \quad \text{(A-6)}$$

Therefore, neglecting the constant term A, and summing up B and C, (7) and (8) follow. To derive (19)–(20) we can further partition C in (A-6) by the expansion of its first addend using steps similar to the ones used to derive (A-5). Adding B to C, we obtain that the metric in (8) can be written as follows:

$$\begin{aligned} \Omega^{u,k,l}(\underline{\hat{a}}) = \mathrm{Re}\Big\{\hat{a}^{u,k}(lT_0)^*\Big(& 2z^{u,k}(lT_0) \\ & - \hat{a}^{u,k}(lT_0)s^{u,u,k,k}(lT_0,\, lT_0) \\ & - 2\sum_{u'<u}\hat{a}^{u',k}(lT_0)s^{u,u',k,k}(lT_0,\, lT_0) \\ & - 2\sum_{u'=1}^{N_U}\sum_{k'<k}\hat{a}^{u',k'}(lT_0)s^{u,u',k,k'}(lT_0,\, lT_0) \\ & - 2\sum_{u'=1}^{N_U}\sum_{k'=1}^{M}\sum_{l'<l}\hat{a}^{u',k'}(l'T_0)s^{u,u',k,k'}(lT_0,\, l'T_0)\Big)\Big\}. \end{aligned} \quad \text{(A-7)}$$

Finally using the index definitions in (12)–(16), we obtain (19) and (20).

References

[1] M. Alard and R. Lassalle, "Principles of Modulation and Channel Coding for Digital Broadcasting for Mobile Receivers," EBU Review, 224 (Aug. 1987), 168–190.

[2] American National Standards Institute, "Network and Customer Installation Interfaces—Asymmetric Digital Subscriber Line (ADSL) Metallic Interface," ANSI T1E1.413, Aug. 1995, <http://www.ansi.org>.

[3] J. B. Anderson and S. Mohan, "Sequential Coding Algorithms: A Survey and Cost Analysis," IEEE Trans. on Commun., 32 (Feb. 1984), 169–176.

[4] S. L. Ariyavisitakul, "Turbo Space-Time Processing to Improve Wireless Channel Capacity," IEEE Trans. on Commun., 48 (Aug. 2000), 1347–1359.

[5] L. R. Bahl, J. Cocke, F. Jelinek, and J. Raviv, "Optimal Decoding of Linear Codes for Minimizing Symbol Error Rate," IEEE Trans. on Information Theory, 20 (Mar. 1974), 284–287.

[6] N. Benvenuto and G. Cherubini, "Algoritmi e circuiti per telecomunicazioni," Libreria Progetto ed., parte seconda, (in Italian), 1999.

[7] C. Berrou, C. A. Glavieux, and P. Thitimajshima, "Near Shannon Limit Error Correcting Coding and Decoding: Turbo Codes," Proc. of IEEE ICC 1993 (Geneva, Switzerland., 1993), pp. 1064–1070.

[8] G. E. Bottomley and S. Chennakeshu, "Unification of MLSE Receivers and Extension to Time-Varying Channels," IEEE Trans. on Commun., 46 (Apr. 1998), 464–72.

[9] G. Caire, G. Taricco, and E. Biglieri, "Bit-Interleaved Coded Modulation," IEEE Trans. on Information Theory, 44:3 (1998), 927–946.

[10] R. W. Chang, "Synthesis of Band-Limited Orthogonal Signals for Multichannel Data Transmission," Bell Sys. Tech. J., 45:10 (1966), 1775–1796.

[11] Q. Chen, Q. E. S. Sousa, and S. Pasupathy, "Multi-Carrier DS-CDMA with Adaptive Sub-Carrier Hopping for Fading Channels," Proc. of PIMRC (Toronto, Can., 1995), pp. 76–80.

[12] G. Cherubini, E. Eleftheriou, E. S. Olcer, and J. M. Cioffi, "Filter Bank Modulation Techniques for Very High-Speed Digital Subscriber Lines," IEEE Commun. Mag., (May 2000), 98–104.

[13] L. Cimini Jr., "Analysis and Simulation of a Digital Mobile Channel Using Orthogonal Frequency Division Multiplexing," IEEE Trans. on Commun., 33 (July 1985), 665–675.

[14] C. Douillard, M. Jezequel, C. Berrou, A. Picart, P. Didier, and A. Glavieux, "Iterative Correction of Intersymbol Interference: Turbo-Equalization", IEE European Trans. on Telecommun., 6 (Sept.–Oct. 1995), 507–511.

[15] European Telecommunications Standards Institute, "Broadband Radio Access Networks (BRAN); HIPERLAN Type 2 Technical Specifications; Physical Layer," (Aug. 1999), <http://www.etsi.org>.

[16] European Telecommunications Standards Institute, "Digital Video Broadcasting: Framing Structure, Channel Coding and Modulation for Digital Terrestrial Television (DVB-T)," Std. ETSI 300 744 (Mar. 1997), <http://www.etsi.org>.

[17] M. V. Eyuboglu and S. U. H. Qureshi, "Reduced-State Sequence Estimation with Set Partitioning and Decision Feedback," IEEE Trans. on Commun., 36 (Jan. 1988), 13–20.

[18] J. Hagenauer, "Iterative Decoding of Binary and Block Convolutional Codes," IEEE Trans. on Information Theory, 42 (Mar. 1996), 429–445.

[19] B. Hirosaki, "An Orthogonally Multiplexed QAM System Using Discrete Fourier Transform," IEEE Trans. on Commun., 29:7 (1981), 982–989.

[20] Institute for Electrical and Electronics Engineers, "Wireless LAN Medium Access Control (MAC) and Physical Layer Specifications: High Speed Physical Layer in the 5 Ghz Band," IEEE 802.11a, (1999), <http://www.ieee.org>.

[21] S. Kaiser and W. Krzymien, "Performance Effects of the Uplink Asynchronism Is a Spread Spectrum Multi-Carrier Multiple Access System," IEE European Trans. on Telecommun., 10 (July–Aug. 1999), 399–406.

[22] K. D. Kammeyer, U. Tuisel, H. Schulze, and H. Bochmann, "Digital Muticarrier-Transmission of Audio Signals over Mobile Radio Channels," IEE European Trans. on Telecommun., 3 (May–June 1992), 23–32.

[23] S. Kondo and L. B. Milstein, "Performance of Multicarrier DS CDMA Systems," IEEE Trans. on Commun., 44 (Feb. 1996), 238–246.

[24] B. Le Floch, R. Halbert-Lassalle, and D. Castelain, "Digital Sound Broadcast to Mobile Receiver," IEEE Trans. on Consumer Electronics, 35:3 (Aug. 1989), 493–503.

[25] M. Moher, "An Iterative Multiuser Decoder for Near-Capacity Communications," IEEE Trans. on Commun., 46 (July 1998), 870–880.

[26] M. Ohkawa, R. Kohno, and H. Imai, "Orthogonal Multicarrier Frequency Hopping-Code Division Multiple Access Scheme for Frequency-Selective Fading," Electronics and Commun. in Japan, Part 1, 78:8 (1995), 86–97.

[27] P. Patel, J. M. Holtzman, "Analysis of a Simple Successive Interference Cancellation Scheme in a DS/CDMA System," IEEE J. on Selected Areas in Commun., 12 (June 1994), 796–807.

[28] T. Pollet, M. Peeters, M. Moonen, and L. Vandendorpe, "Equalization for DMT-Based Broadband Modems," IEEE Commun. Mag., (May 2000), 106–113.

[29] J. G. Proakis, Digital Communications, 3rd ed., New York, McGraw-Hill, 1995.

[30] M. Speth, S. A. Fechtel, G. Fock, and H. Meyer, "Optimum Receiver Design for Wireless Broadband Systems Using OFDM—Part I," IEEE Trans. on Commun., 47 (Nov. 1999), 1668–1677.

[31] M. Speth, S. A. Fechtel, G. Fock, and H. Meyer, "Optimum Receiver Design for OFDM-Based Broadband Transmission—Part II: A Case Study," IEEE Trans. on Commun., 49 (April 2001), 571–578.

[32] V. Tarokh, N. Seshadri, and A. R. Calderbank, "Space-Time Codes for High Data Rate Wireless Communication: Performance Criterion and Code Construction," IEEE Trans. on Information Theory, 44 (Mar. 1998), 744–765.

[33] A. M. Tonello, "Array Processing for Simplified Turbo Decoding of Interleaved Space-Time Codes," Proc. of IEEE Vehicular Technology Conf. (Atlantic City, NJ, 2001), pp. 1304–1308.

[34] A. M. Tonello, "Iterative MAP Detection of Coded M-DPSK Signals in Fading Channels with Application to IS-136 TDMA," Proc. of IEEE Vehicular Technology Conf. (Amsterdam, Netherlands, 1999), pp. 1615–1619.

[35] A. M. Tonello, "Multicarrier Multiuser Asynchronous Communications," Doctor of Research Degree Thesis, Università di Padova, 2001.

[36] A. M. Tonello, "On Turbo Equalization of Interleaved Space-Time Codes," Proc. of IEEE Vehicular Technology Conf. (Atlantic City, NJ, 2001), 887–891. To appear also in IEEE Trans. On Commun., 2002.

[37] A. M. Tonello, "Performance Limits of Multicarrier-Based Systems in Fading Channels with Optimal Detection," to appear in Proc. of IEEE Wireless Personal Multimedia Commun. Symposium (Honolulu, HI, 2002).

[38] A. M. Tonello, "Space-Time Bit-Interleaved Coded Modulation with an Iterative Decoding Strategy," Proc. of IEEE Vehicular Technology Conf. (Boston, MA, 2000), pp. 473–478.

[39] A. M. Tonello, N. Laurenti, and S. Pupolin, "Analysis of the Uplink of an Asynchronous DMT OFDMA System Impaired by Time Offsets, Frequency Offsets, and Multi-Path Fading," Proc. of IEEE Vehicular Technology Conf. (Boston, MA, 2000), pp. 1094–1099.

[40] A. M. Tonello, N. Laurenti, and S. Pupolin, "Capacity Considerations on the Uplink of a Multi-User DMT OFDMA System Impaired by Time Misalignments and Frequency Offsets," Proc. of 12th Tyrrhenian Workshop on Digital Commun.—Software Radio Technologies and Services, Springer-Verlag (Portoferraio, Isola D'Elba, 2000), pp. 93–104.

[41] A. M. Tonello, N. Laurenti, and S. Pupolin, "On the Effect of Time and Frequency Offsets in the Uplink of an Asynchronous Multi-User DMT OFDMA System," Proc. of Intl. Conf. on Telecommun. (Acapulco, Mex., 2000), pp. 614–618.

[42] A. M. Tonello and S. Pupolin, "Discrete Multi-Tone and Filtered Multi-Tone Architectures for Broadband Asynchronous Multi-User Communications," Proc. of Wireless Personal Multimedia Commun. Symposium (Aalborg, Den., 2001), pp. 461–466.

[43] A. M. Tonello and S. Pupolin, "Performance of Single-User Detectors in Multitone Multiple Access Asynchronous Communications," Proc. of IEEE Vehicular Technology Conf. (Birmingham, AL, 2002), pp. 199–203.

[44] G. Ungerboeck, "Adaptive Maximum Likelihood Receiver for Carrier-Modulated Data Transmission Systems," IEEE Trans. on Commun., 22 (May 1974), 624–636.

[45] J. Van de Beek, P. O. Borjesson, M. L. Boucheret, D. Landstrom, J. M. Arenas, P. Odling, C. Ostberg, M. Wahlqvist, and

S. K. Wilson, "A Time and Frequency Synchronization Scheme for Multiuser OFDM," IEEE J. on Selected Areas in Commun., 17 (Nov. 1999), 1900–1914.

[46] V. Van Etten, "Maximum Likelihood Receiver for Multiple Channel Transmission Systems," IEEE Trans. on Commun., 24 (Feb. 1976), 276–283.

[47] L. Vanderdorpe, "Multitone Spread Spectrum Multiple Access Communications System in a Multipath Rician Fading Channel," IEEE Trans. on Vehicular Technology, 44 (May 1995), 327–337.

[48] M. K. Varanasi and B. Aazhang, "Multistage Detection in Asynchronous Code-Division Multiple-Access Communications," IEEE Trans. on Commun., 38 (Apr. 1990), 509–519.

[49] S. Verdu, "Minimum Probability of Error for Asynchronous Gaussian Multiple-Access Channels," IEEE Trans. on Information Theory, 32 (Jan. 1986), 85–96.

[50] L. Wei and C. Schlegel, "Synchronization Requirements for Multi-User OFDM on Satellite Mobile and Two-Oath Rayleigh Fading Channels," IEEE Trans. on Commun., 43 (Feb.–Apr. 1995), 887–895.

[51] S. B. Weinstein and P. M. Ebert, "Data Transmission by Frequency-Division Multiplexing Using the Discrete Fourier Transform," IEEE Trans. on Commun. Tech., 19:5 (1971), 628–634.

(Manuscript approved September 2002)

ANDREA M. TONELLO is a technical manager in the

Wireless Advanced Technology Department at Bell Labs in Whippany, New Jersey, and the managing director of Bell Labs Italy. He received both the Doctor of Engineering degree in electronics (cum laude) and the Doctor of Research degree in electronics and telecommunications from the University of Padova in Italy. Dr. Tonello conducts research on wireless systems with emphasis on air interface design and performance analysis, and he is also responsible for fostering research initiatives with industrial and academic institutions. ◆